Of many chemicals that bind to AhR, TCDD is a well-known ligand having high affinity and eliciting potent suppressive effect on both humoral and cell-mediated immune responses (Holsapple et al., 1991; Nohara et al., 2002; Kerkvliet, 2003; Inouye et al., 2003; Lawrence and Kerkvliet, 2007). Recent studies have shown that AhR activation by TCDD enhances expansion of $CD4^+CD25^+$ cells, particularly $CD62L^{low}CD4^+CD25^+$ cells, and $CD4^+Foxp3^+$ regulatory T-(Treg) cells (Funatake et al., 2005; Quintana et al., 2008). AhR activation also participates in Th17 differentiation (Quintana et al., 2008; Kimura et al., 2008; Veldhoen et al., 2008). Thus, Ahr is involved in a variety of immune responses and suppressions, while the mechanism is not fully understood.

In attempts to clarify the target cells affected by AhR activation, previous studies have shown that T-cells are direct AhR-dependent targets of TCDD-mediated immune suppression, and both $CD4^+$ and $CD8^+$ T-cells must express AhR in order for full suppression of the CTL response to alloantigen (Kerkvliet et al., 2002). Subsequent studies showed that activation of AhR in the donor T-cells was also required for TCDD-mediated induction of a subpopulation of T-cells that are $CD25^{hi}CD62L^{low}$ and exhibit suppressive activity *in vitro*, for both $CD4^+$ (Funatake et al., 2005) and $CD8^+$ T-cells (Funatake et al., 2008). However, many other cells in the immune system express AhR and are also known to be directly targeted by TCDD, including dendritic cells and B-cells (Sulentic et al., 1998; Vorderstrasse and Kerkvliet, 2001; Boverhof et al., 2004; Ruby et al., 2005). A recent study has shown that activation of AhR within hematopoietic cells, but not within $CD8^+$ T-cells, is necessary for suppression of the CTL response to influenza, suggesting that in the influenza model, the immunosuppressive effects of TCDD are mediated by the activation of AhR in immune cells other than the responding $CD8^+$ T-cells (Lawrence et al., 2006). Thus, although studies have shown that activation of AhR within the donor T-cells is required for suppression of the CTL response to alloantigen, it is not known if activation of AhR in T-cells alone is sufficient to mediate this suppression.

In order to address the exact role of the AhR in T-cells, we previously-produced transgenic (Tg) mice expressing a constitutively active AhR (CA-AhR) under the control of the T-cell lineage-specific CD2 promoter (Nohara et al., 2005). These mice express the transgene in their thymocytes, CD4 T-cells, and CD8 T-cells, and they express CYP1A1 mRNA in the thymus and spleen, showing that the CA-AhR is transcriptionally active in T-cells. These mice also display thymic atrophy (Nohara et al., 2005), which is one of the hallmarks of exposure to TCDD that occurs in an AhR-dependent manner (Laiosa et al., 2003). The immune response of these mice against Ovalbumin (OVA)-alum only partially mimicked the immune response of wild-type mice exposed to TCDD (Nohara et al., 2005, 2009). For example, splenocytes from CA-AhR Tg mice produced levels of interleukin (IL)-4 and IL-5 and antibody titers upon OVA immunization similar to those of wild-type mice (Nohara et al., 2009).

On the other hand, interferon (IFN)-γ production by the splenocytes upon OVA immunization was augmented in the Tg mice similar to that seen in wild-type mice exposed to TCDD (Nohara et al., 2009). In the present study, we used the transgenic CA-AhR mice to ask whether activation of AhR in T-cells alone was sufficient to induce the $CD25^+CD62L^{low}$ adaptive Treg-like phenotype and mediate suppression of the CTL response to alloantigen. To do so, we compared the response of CA-AhR-expressing B6 donor T-cells in B6xD2F1 mice and the response of wild-type B6 donor T-cells in B6xD2F1 mice given a single dose of TCDD in the acute graft-versus-host (GVH) model.

Materials and methods

Mice and treatment with TCDD

The generation and genotyping of the transgenic C57Bl/6-CA-AhR (CA-AhR) mice has been described (Nohara et al., 2005). The heterozygous Tg mice showed CYP1A1 mRNA expression in the thymus at the level corresponding approximately to the level induced by a single dose of 20 μg TCDD/kg (Nohara et al., 2005). The transgenic CA-AhR mice and wild-type (B6-WT) littermates used in the present studies were backcrossed to the B6 background over 10 generations. For some GVH experiments, transgenic CA-AhR mice ($CA\text{-}AhR^{+/-}$) were crossed with B6.PL-$Thy1^a$/CyJ (Thy1.1) mice, purchased from The Jackson Laboratory (Bar Harbor, ME), to generate $Thy1.1^+$ donor T-cells. $Thy1.1^+$ $CA\text{-}AhR^{-/-}$ littermates were used as B6-WT controls. B6D2F1/Crlj mice were purchased from Charles River Laboratories (Yokohama, Japan).

B6D2F1/J mice were generated by breeding C57Bl/6J female mice with DBA/2J male mice, originally purchased from CLEA Japan (Tokyo). In one study, B6 mice lacking AhR (AhrΔ2; Schmidt et al., 1996) were crossed with DBA/2 mice, (both purchased from The Jackson Laboratory). All mice were used between 2 and 5 months of age. Except where noted, B6D2F1 mice were dosed orally with 20 μg TCDD/kg body weight 1 day before the injection of donor T-cells, as previously described (Kerkvliet et al., 2003). TCDD was purchased from Cambridge Isotope Laboratories (Andover, MA) and prepared as a 4% nonane/corn oil solution. A similarly prepared solution of 4% nonane in corn oil was used as a vehicle-control. All mice were handled in a humane manner in accordance with the National Institute for Environmental Studies (NIES, Japan) guidelines for animal experiments.

Preparation of donor T-cells for the GVH model

T-Cells were purified from spleen cells of B6-WT or transgenic CA-AhR mice using the BD IMag™ and a mouse T-lymphocyte enrichment set (BD Biosciences, San Jose, CA), following the manufacturer's instructions. The percentages of $CD4^+$ and $CD8^+$ cells in the T-cell fraction were checked using flow cytometry (see below for details) and viability was assessed by trypan blue exclusion. T-Cells (i.e., $CD4^+$ and $CD8^+$ cells) were 80-93% pure and viabilities were > 90%.

The concentration of purified T-cells was adjusted so that each F1 mouse received 1.5×10^7 T-cells intravenously in 250 μl of 1X Hank's Balanced Salt Solution (HBSS). B6-WT mice were used as syngeneic recipients. In some experiments the purified donor T-cells were labeled with 0.5 μM Carboxyfluorescein Succinimydl Ester (CFSE) (Invitrogen, Carlsbad, CA) before injection into F1 or syngeneic hosts as described previously (Funatake et al., 2004).

Flow cytometry

Spleen cells were resuspended in staining buffer containing 0.1% sodium azide and 1% fetal bovine serum in phosphate-buffered saline. The cells were incubated with 200 μg/ml rat IgG (Jackson Immunoresearch, West Grove, PA) to block F_c receptors (F_cR), followed by incubation with fluorochrome- or biotin-conjugated monoclonal antibodies. Antibodies for Thy1.1, CD4, CD62L, CD19, and CD25 were purchased from eBiosciences (San Diego, CA). All other antibodies were purchased from BD Biosciences. After incubation with monoclonal antibodies, the cells were washed and incubated with streptavidin conjugated to allophycocyanin, PerCP (BD Biosciences), or PE-Cy5 (eBiosciences). After incubating the cells with streptavidin, the cells were washed and resuspended in staining buffer, and data were collected on 7000-10,000 events of interest using a BD FACSCalibur (BD Biosciences). Data were analyzed using CellQuest software (BD Biosciences).

Cytotoxicity assay

With one noted exception that used the standard ^{51}Cr-release assay, spleen cells were assayed for CTL activity using the CytoTox 96® non-radioactive cytotoxicity assay kit from Promega (Madison, WI), according to the manufacturer's instructions. Briefly, P815 cells recovered from the ascites of DBA/2 mice were added to a 96-well round bottom plate at 1×10^4/well. Spleen cells from F1 mice that had been injected with B6 donor T-cells 10 days earlier were then added to the wells in duplicate serial dilutions from 100:1 to 12.5:1. Wells containing only spleen cells were included as background controls, in addition to wells containing only P815 cells with or without lysis buffer used for maximum and spontaneous release controls, respectively. The plates were incubated for 4 hr at 37°C and 5% CO_2, after which the CTL activity was measured and the percent cytotoxicity was calculated according to the manufacturer's instructions.

7-Ethoxyresorufin-O-deethylase (EROD) activity assay

Livers were homogenized and debris was removed by centrifugation at 10,000x*g* for 20 min at 4°C. The microsomal fraction was isolated from the supernatants by additional centrifugation at 100,000x*g* for 90 min at 4°C. The EROD activity of each microsomal fraction was determined using 2 μg of protein for the WT-F1 samples and 25 μg for the KO-F1 ($AhR^{-/-}$ B6 mice bred with DBA/2 mice to create F1 hosts that would respond poorly to AhR activation) samples. Microsomal protein was aliquoted into microtiter wells containing 200 μM 7-ethoxy-resorufin in 0.1M Tris-HCl, (pH 7.8.) NADPH was added to each well and the fluorescence was measured on a SpectraMAX Gemini plate reader using 535 nm excitation and 585 nm emission filters. Samples were assayed in triplicate and the amount of resorufin produced was calculated using a resorufin standard curve.

Statistics

All experiments were independently conducted twice with n = 3-5 mice per group per experiment. Where appropriate, data from replicate studies were combined, and all data are presented as the mean ± SEM. The differences between means were analyzed by Student's *t*-test, with $p < 0.05$ considered statistically significant.

Results

CA-AhR does not affect cell division or the number of donor T-cells in the spleen on Day 2

Previous studies have shown that exposure of F1 mice to TCDD has no adverse effect on the proliferation or number of donor T-cells in the spleen on Day 2 of the GVH response (Funatake et al., 2005, 2008). To determine if expression of CA-AhR in donor T-cells affected cell division or cell number in the spleen, we compared donor T-cells from transgenic CA-AhR mice to donor T-cells from B6-WT mice two days after injection into vehicle- or TCDD-treated F1 hosts. Donor T-cells from CA-AhR mice or wild-type littermates were labeled with CFSE before injection into F1 hosts for evaluation of cell division. As with TCDD, CA-AhR in the donor T-cells had no effect on the total number of spleen cells (Figure 1A) or on the number of donor $CD4^+$ T-cells in the spleen on Day 2 (Figure 1B). In addition, neither exposure to TCDD nor CA-AhR had any effect on the cell division of donor $CD4^+$ T-cells (Figure 1D). Exposure to TCDD led to a small but significant increase in the number of donor $CD8^+$ T-cells (Figure 1C), and there was a corresponding increase in the percentage of donor $CD8^+$ T-cells that had undergone one or more cell divisions (Figure 1E, middle panel). CA-AhR in the donor T-cells had no effect on the number of donor $CD8^+$ T-cells in the spleen (Figure 1C) or on the percentage of donor $CD8^+$ cells that were dividing (Figure 1E). As expected, in syngeneic B6 recipients, there was no difference in the total number of spleen cells or the number of donor $CD4^+$ or $CD8^+$ T-cells in the spleen two days after injection of donor T-cells from either B6-WT or CA-AhR mice (Figure 1).

CA-AhR enhances the down-regulation of CD62L but does not affect the expression of CD25

Next, we compared the effect of the CA-AhR to the effect of TCDD on the expression of CD25 and CD62L on the donor $CD4^+$ and $CD8^+$ T-cells. For donor $CD4^+$ T-cells, exposure to TCDD caused a large increase in the percentage of cells expressing CD25, whereas CA-AhR had a much more modest effect (Figure 2A and 3A). In contrast, both activation of AhR by TCDD and CA-AhR caused a substantial increase in the percentage of donor $CD4^+$ T-cells that had down-regulated CD62L (Figure 2C and 3A). For donor $CD8^+$ T-cells,

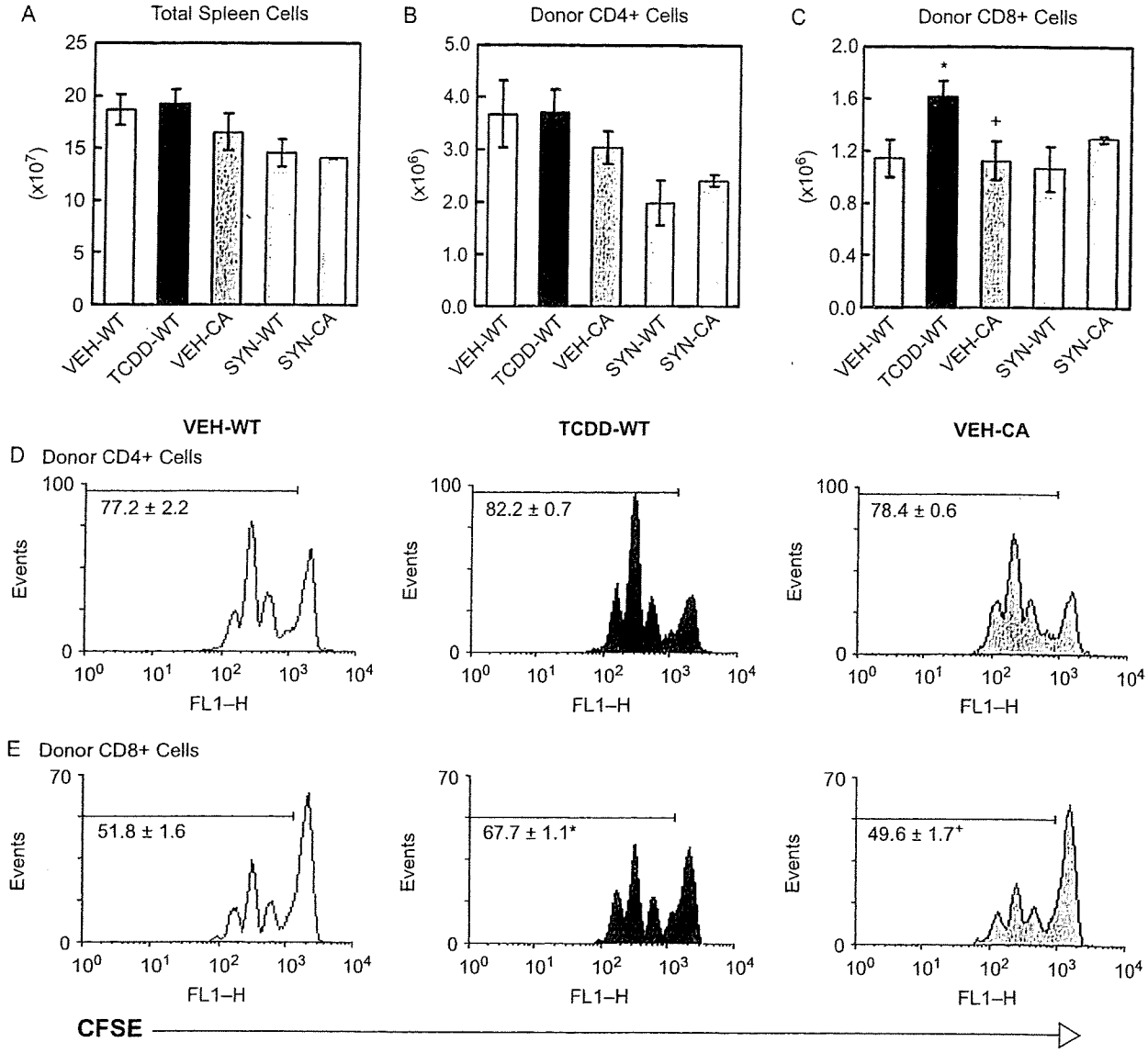

Figure 1. CA-AhR does not alter the number or proliferation of donor T-cells in the spleen on Day 2. Age- and gender-matched F1 mice were dosed with vehicle or 20 μg/kg TCDD one day before the injection of donor T-cells from B6-WT or CA-AhR mice. On Day 2 after injection of donor T-cells, the spleens from F1 mice were collected and analyzed by flow cytometry. After gating on total spleen cells (A), the donor T-cells were identified as $CFSE^+CD4^+$ (B) or $CFSE^+CD8^+$ (C). For A-C, data are combined from two independent experiments and n = 4-6 mice per group. VEH, vehicle-treated F1 recipient; TCDD, TCDD-treated F1 recipient; SYN, syngeneic B6 recipient; WT, donor T-cells from wild-type mice; CA, donor T-cells from CA-AhR Tg mice. The percentage of donor $CD4^+$ (D) or $CD8^+$ T-cells (E) that were dividing was determined on Day 2. Representative histograms are shown and the numbers on the histograms indicate the mean ± SEM of the percentage of cells in divisions 1-4 for n = 3 mice per group. *Indicates statistically significant difference compared to VEH-WT; +indicates statistically significant difference compared to TCDD-WT.

a similar phenomenon was seen. Exposure to TCDD dramatically increased the frequency of CD25-expressing cells while CA-AhR produced only a slight increase (Figure 2B and 3B). Additionally, both TCDD and CA-AhR increased the frequency of donor $CD8^+$ T-cells that had down-regulated CD62L (Figure 2D and 3B). The decrease in CD62L occurred stepwise as the T-cells divided, as indicated by the decrease in median fluorescence intensity for both TCDD-treated and CA-AhR-expressing donor T-cells as compared to vehicle-treated donor T-cells (Figures 2E and 2F). Interestingly, in syngeneic recipients, CA-AhR also caused a small increase in the frequency of donor T-cells that had down-regulated CD62L as compared to B6-WT donors for both $CD4^+$ and $CD8^+$ T-cells (Figures 2C and 2D, light grey bars).

Expression of $CD25^{hi}CD62L^{low}$ Treg phenotype

Recently, we reported that a subpopulation of donor $CD4^+$ T-cells in TCDD-treated mice is $CD25^{hi}CD62L^{low}$ and that this subpopulation has Treg-like suppressive activity *in vitro* (Funatake et al., 2005). We have also observed the same phenotype and *in vitro* suppressive activity for donor $CD8^+$ T-cells from TCDD-treated mice (Funatake et al., 2008). However, as shown above, for donor T-cells expressing CA-AhR, there were only minor changes in the expression of CD25 while at

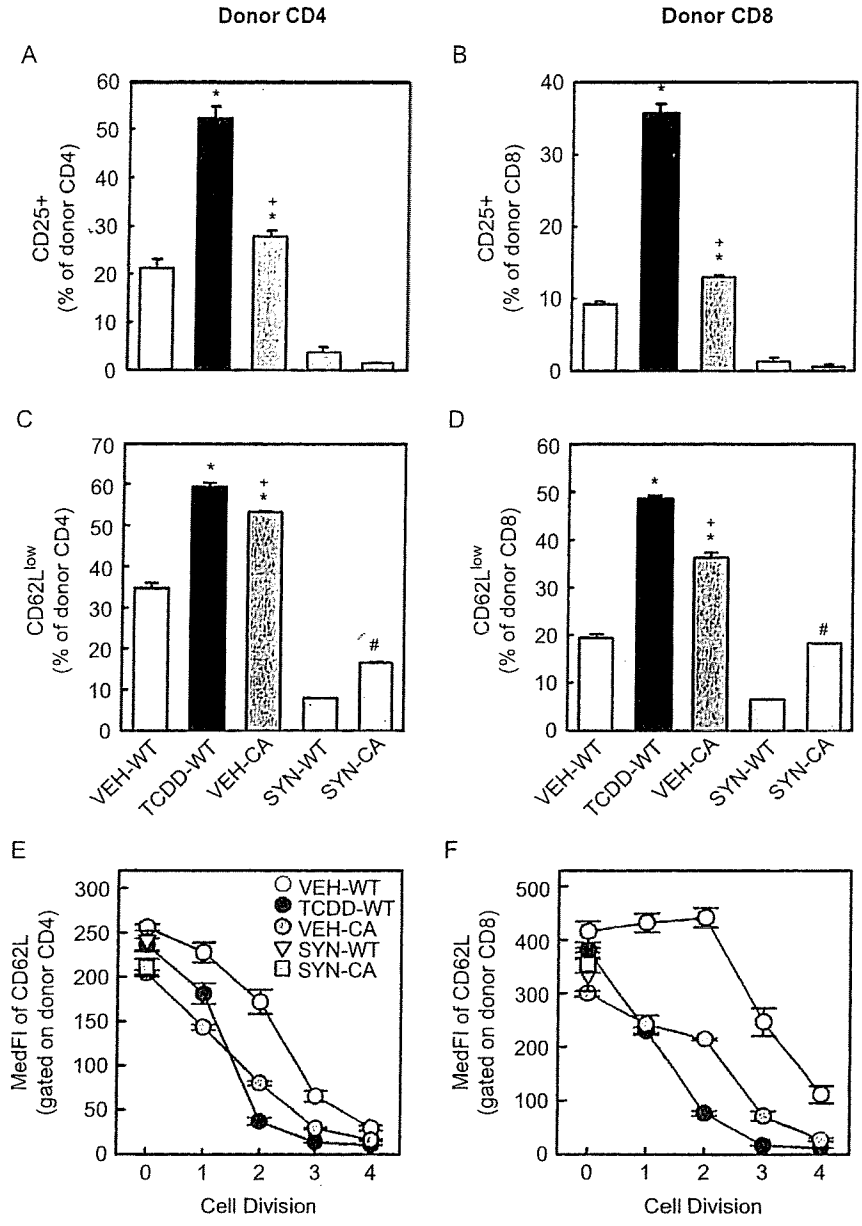

Figure 2. CA-AhR enhances the down-regulation of CD62L comparable to TCDD but has only a minimal effect on the up-regulation of CD25. F1 mice were treated with vehicle or TCDD as described for Figure 1. On Day 2, the donor CD4⁺ (A and C) and donor CD8⁺ T-cells (B and D) were analyzed for the expression of CD25 (A and B) and CD62L (C and D). For CD25, data are combined from two independent experiments with n = 4-6 mice per group. For CD62L, data are from a representative experiment with n = 3-4 mice per group. Also on Day 2, the median fluorescence intensity (MedFI) of CD62L was determined for each cell division for donor CD4⁺ (E) and CD8⁺ (F) T-cells. *Indicates statistically significant difference compared to VEH-WT; ⁺indicates statistically significant difference compared to TCDD-WT; #indicates statistically significant difference compared to SYN-WT.

the same time expression of CD62L was profoundly down-regulated. When we examined the co-expression of these two markers on the donor T-cells two days after injection into F1 hosts, exposure to TCDD greatly increased the percentage of cells that were $CD25^{+}CD62L^{low}$ for both donor $CD4^{+}$ and $CD8^{+}$ T-cells (Figures 3A and 3B, middle panel) In contrast, donor T-cells expressing CA-AhR exhibited a significant but much smaller increase in the percentage of donor $CD4^{+}$ or $CD8^{+}$ T-cells that were $CD25^{+}CD62L^{low}$ when compared to vehicle-treated mice (Figures 3A and 3B, right panel). Thus, compared to the effect from TCDD treatment, CA-AhR in the donor T-cells alone does not appear to be sufficient to induce a subpopulation of $CD25^{hi}CD62L^{low}$ donor T-cells.

Development of effector CTL and CTL activity is not impaired by CA-AhR

To determine if CA-AhR in T-cells alone was sufficient to suppress the CTL response, we injected F1 mice with donor T-cells from B6-WT or transgenic CA-AhR mice and 10 days later tested the spleen cells from F1 mice for the presence of effector CTL and CTL activity. As shown in Figure 4A, there were significantly more spleen cells in TCDD-treated

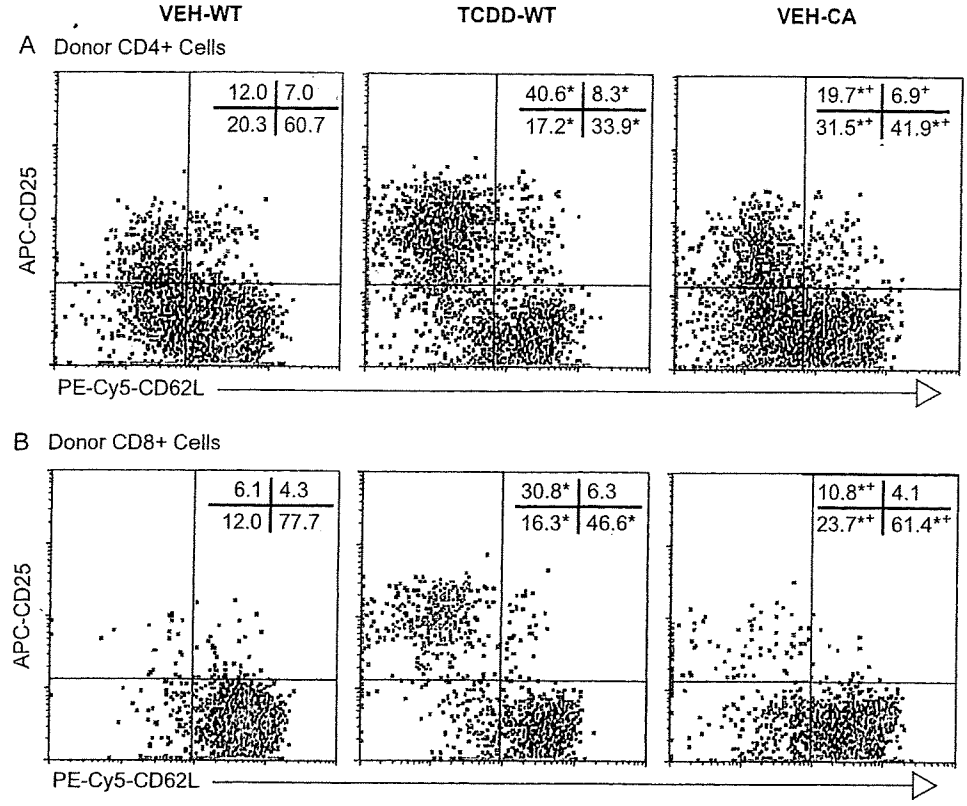

Figure 3. CA-AhR does not expand a subpopulation of $CD25^{hi}CD62L^{low}$ donor T-cells. F1 mice were treated with vehicle or TCDD as described for Figure 1. The co-expression of CD25 and CD62L was determined for the donor $CD4^+$ (A) and donor $CD8^+$ T-cells (B) on Day 2. Representative histograms are shown and the numbers on the histograms indicate the mean of the percentage of cells in each quadrant for n = 3 mice per group (SEM is excluded for clarity). *Indicates statistically significant difference compared to VEH-WT; +indicates statistically significant difference compared to TCDD-WT.

mice, while CA-AhR in the donor T-cells had no effect on the number of spleen cells on Day 10. The greater number of total spleen cells in TCDD-treated mice on Day 10 was due to greater numbers of host B-cells and host T-cells in the spleen reflecting the absence of an anti-host immune response, as shown in Figures 4D-4F. In addition, the number of donor $CD4^+$ and donor $CD8^+$ T-cells in the spleen was greatly reduced in TCDD-treated mice, while CA-AhR had no effect on the number of donor T-cells compared to vehicle-treated controls (Figures 4B and 4C).

Of the few donor $CD8^+$ T-cells present in the spleen of TCDD-treated mice on Day 10, significantly fewer expressed an effector CTL phenotype ($CD44^{hi}CD62L^{low}$) as compared to donor $CD8^+$ T-cells in vehicle-treated controls (Figure 5B), resulting in essentially no effector CTL present in the spleens of TCDD-treated mice (Figure 5C). In mice receiving CA-AhR donor T-cells, there was no difference in the percentage or number of donor-derived effector CTL as compared to vehicle-treated F1 mice that received WT donor T-cells (Figures 5B and 5C).

On Day 10, CTL activity in the spleen was measured *ex vivo* in a 4-hour non-radioactive cytotoxicity assay, as described in the Methods, and the percentage and number of effector CTL was determine by flow cytometry. As shown in Figure 5A, no CTL activity was detected with splenocytes from TCDD-treated mice. In contrast, the CTL activity of spleen cells from mice injected with CA-AhR donor T-cells was indistinguishable from CTL activity in vehicle-treated mice injected with WT donor T-cells (Figure 5A). Together, these data suggest that AhR activation only in T-cells is not sufficient to suppress CTL activity in the GVH model.

Influence of AhR responsiveness of F1 host mice on donor CTL activity

The absence of an expanded population of $CD25^{hi}CD62L^{low}$ donor T-cells and the lack of suppression of effector CTL when the donor T-cells expressed CA-AhR might suggest that activation of AhR in donor T-cells only is not sufficient to suppress the CTL response, and that activation of AhR in host cells (e.g., dendritic cells that activate the donor T-cells) contribute to the suppression of the GVH response by TCDD. To test this hypothesis, we bred $AhR^{-/-}$ B6 mice with DBA/2 mice to create F1 host mice that would respond poorly to AhR activation ("KO-F1"). If AhR activation in host cells contributes to suppression of the donor CTL response by TCDD, the CTL response should be less affected by TCDD in the KO-F1mice.

To confirm the low responsiveness of these KO-F1 mice, we measured EROD activity of CYP1A1 in the liver after treatment with TCDD. WT-F1 mice reached near-maximal EROD activity with as little as 3 μg TCDD/kg body weight, but little to no EROD activity was detected in KO-F1 mice at this dose (Figure 6A). At 15 μg TCDD/kg body weight, a dose previously shown to completely suppress the GVH CTL

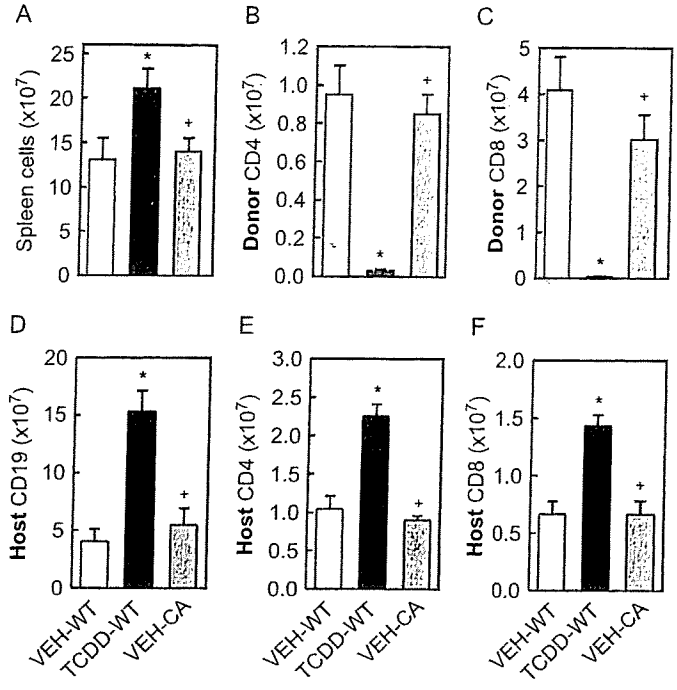

Figure 4. Analysis of the distribution of spleen cells on Day 10 after injection of donor T-cells. F1 mice were treated with vehicle or TCDD as described for Figure 1. On Day 10 after injection of donor T-cells, total spleen cells from F1 mice were counted (A) and analyzed by flow cytometry for enumeration of donor $CD4^+$ (B) and donor $CD8^+$ T-cells (C), host $CD19^+$ cells (D), host $CD4^+$ (E) and host $CD8^+$ T-cells (F). Data from a representative experiment are shown with n = 4-5 mice per group. *Indicates statistically significant difference compared to VEH-WT; +indicates statistically significant difference compared to TCDD-WT.

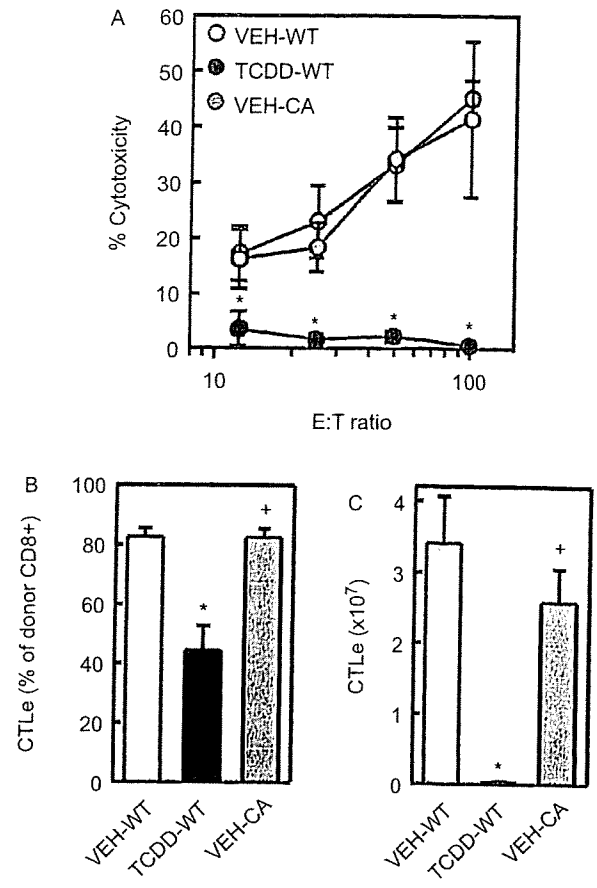

Figure 5. CA-AhR does not suppress the CTL activity or the percentage and number of CTL effectors in the spleen on Day 10. F1 mice were treated with vehicle or TCDD as described for figure 1. Ten days after in the injection of donor T-cells, the spleen cells from F1 mice were tested for CTL activity using a non-radioactive cytotoxicity assay, as described in the Methods (A). The percentage (B) of donor $CD8^+$ cells, identified as $Thy1.1^+CD8^+$ cells, expressing a CTL effector (CTLe) phenotype, defined as $CD44^{hi}CD62L^{low}$, and the number (C) of CTLe in the spleen were determined by flow cytometry. Data from a representative experiment are shown with n = 4-5 mice per group. *Indicates statistically significant difference compared to VEH-WT; +indicates statistically significant difference compared to TCDD-WT.

response (Kerkvliet et al., 2002), the EROD activity in KO-F1 mice was nearly 4 times lower than in WT-F1 mice; even at 30 μg TCDD/kg body weight, the EROD activity of KO-F1 mice was significantly less than in WT-F1 mice (Figure 6A).

Interestingly, despite the low host response to TCDD, the CTL response of AhR-WT donor T-cells in KO-F1 hosts was suppressed by TCDD to the same extent as in WT-F1 hosts (Figure 6B), suggesting that activation of AhR in host cells plays a minimal role in mediating the suppressive effects of TCDD in this model. These data suggest that CA-AhR does not behave the same as ligand (TCDD)-bound AhR in T-cells that appears to be necessary and sufficient for suppressing the CTL response. However, it remains possible that even low-level activation of AhR within key cells of the KO-F1 host treated with 15 μg/kg TCDD was sufficient to synergize with AhR-mediated signaling in T-cells to suppress the CTL response. Additional studies will be necessary to determine which of these interpretations is correct.

Discussion

In the present study, we used transgenic mice that express CA-AhR only in T-lineage cells (Nohara et al., 2005). The CA-AhR mutant has a minimal deletion in the PAS B domain which is required for binding to hsp90 and also contains part of the ligand binding domain. The minimal deletion causes the AhR to localize in the nucleus, heterodimerize with ARNT, and activate transcription by binding DRE sequences in a ligand-independent manner (McGuire et al., 2001).

In our recent study (Nohara et al., 2009), we found that CA-AhR Tg mice elicit the same level of IL-4 and IL-5 production and antibody production upon OVA immunization as wild-type mice do. We showed in the present study that CA-AhR T-cells normally proliferate and differentiate into CTL effector cells with CTL activity in B6D2F1 hosts as wild-type B6 cells. In CA-AhR Tg mice, CA-AhR is expressed in the T-cells from their fetal stage, which might affect the immune function (Nohara, et al., 2005). Nevertheless, the results obtained so far indicate that the immune system of Tg mice still maintains its normal ability to perform humoral and cellular immune responses. The findings appear to be consistent with the fact that other studies have shown that T-cells must be activated in order to see any AhR-dependent changes in phenotype or function (Shepherd et al., 2000;

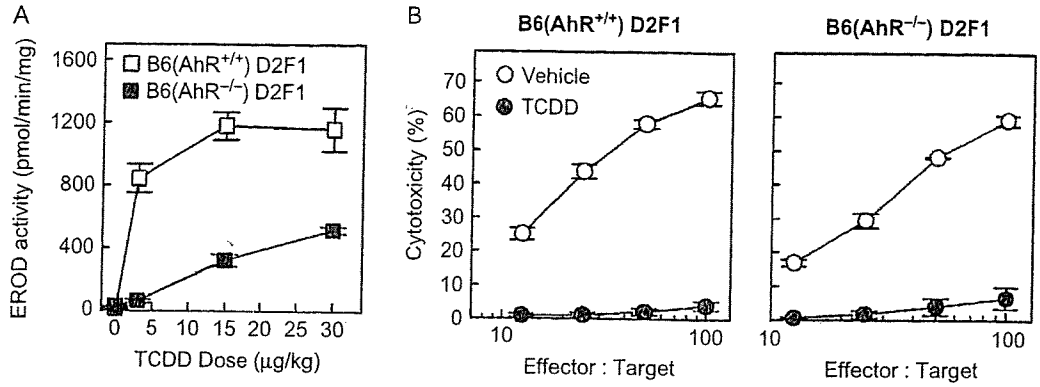

Figure 6. Host AhR does not appear to be involved in suppression of the CTL response on Day 10. (A) KO-F1 and WT-F1 mice were dosed with 0, 3, 15, or 30 μg TCDD/kg body weight and, two days later, the livers were collected and EROD activity was determined as described in the Methods. (B) KO- and WT-F1 mice received AhR-WT donor T-cells and treated with 15 μg TCDD/kg body weight. Ten days later, the CTL activity in the spleen was assessed. Data from a representative experiment are shown.

Funatake et al., 2004). On the other hand, Tg mice develop thymus atrophy (Nohara et al., 2005) and, upon OVA immunization, they showed augmented IFNγ production compared to wild-type mice (Nohara et al., 2009). These changes are also observed in wild-type mice given a single dose of TCDD (Nohara et al., 2005, 2009). The results of the present study show that CA-AhR enhanced the down-regulation of CD62L to the same extent as exposure to a single dose of TCDD (20 μg/kg body weight). Thus, CA-AhR Tg mice show an immune profile, some of which is similar to those of wild-type mice and some of which mimic those observed in wild-type mice given a single dose of TCDD.

In this study, we show that restricting the expression of CA-AhR to T-cells only partially mimics the effects of TCDD in the GVH response. Specifically, CA-AhR enhanced the down-regulation of CD62L, but had no effect on the expression of CD25 and did not suppress CTL activity on Day 10. In previous studies, the down-regulation of CD62L was found to depend strictly on expression of AhR within the affected T-cell population, whereas the up-regulation of CD25, at least for donor $CD8^+$ T-cells, was found to depend indirectly on AhR within the donor $CD4^+$ T-cells (Funatake et al., 2008). Sun et al. (2004) performed a genome-wide study of DRE located between -5000 and +2000 bp for over 11,000 mouse genes and identified eight putative DRE in the promoter region of the gene for CD62L. Three of these putative DRE had match scores equivalent to confirmed DRE for CYP1A1; interestingly, no DRE were identified in the *Il2ra* gene. Together, these findings suggest that CD62L could be a direct target of the AhR-ARNT complex, while CD25 may be an indirect target, dependent on other AhR-ARNT-regulated genes.

It is interesting that although CA-AhR had a profound effect on the down-regulation of CD62L, this did not appear to have any effect on the final outcome of the GVH response, since the CTL activity on Day 10 was unimpaired. CD62L is important for allowing entry of naïve T-cells into the lymph node through the high endothelial venules (Arbones et al., 1994; Bradley et al., 1994; Warnock et al., 1998). Once activated, T-cells down-regulate CD62L; however, this down-regulation is not necessary for the cells to exit out of a lymph node, and is more important for preventing the re-entry of activated T-cells into lymph nodes (Galkina et al., 2003). Some studies have suggested that signaling through CD62L induces conformational changes in integrins and alters expression of chemokine receptors that enhance/prolong the interaction between T-cells and antigen-presenting cells (Giblin et al., 1997; Ding et al., 2003). However, other studies have shown that the lack of CD62L has no adverse effects on the development of autoimmune diabetes (Friedline et al., 2002; Mora et al., 2004). This latter finding is consistent with our results showing that CTL activity is unimpaired on Day 10 of the GVH response despite the enhanced down-regulation of CD62L on donor T-cells expressing CA-AhR. Thus, although AhR may directly target CD62L and induce its down-regulation, this alone is not sufficient for suppression of effector function.

CA-AhR expressed in T-cells did not suppress the GVH response, suggesting that activation of AhR in other immune cells is involved in the immunosuppressive effects of TCDD. In the GVH response, host cells, in particular dendritic cells, contribute to the T-cell response by acting as antigen presenting cells. Previous studies have shown that dendritic cells, like T-cells, are sensitive, AhR-dependent targets of TCDD (Vorderstrasse and Kerkvliet, 2001; Vorderstrasse et al., 2003; Ruby et al., 2005). In order to assess the contribution of host-expressed AhR, $AhR^{-/-}$ B6 mice were crossed with D2 mice to generate KO-F1 hosts with low responsiveness to AhR. If the host AhR contributes significantly to the suppression of the CTL response, we would expect that the CTL activity in these KO-F1 mice to be less sensitive to suppression by TCDD. However, we found that the CTL activity was suppressed to the same extent as in wild-type F1 mice. This would imply that activation of AhR in dendritic cells or other host cells does not have a major influence on the outcome of the T-cell response in this GVH model. One caveat to this interpretation is that there was still activation of AhR, albeit at a much lower level, in the KO-F1 hosts at the dose of TCDD used. This leaves open the possibility that low-level activation of AhR within the host is sufficient to synergize

with the activation of AhR within the donor T-cells, leading to the full suppression of the CTL response. To assess this possibility, generation of $AhR^{-/-}$ B6xAhR$^{-/-}$ D2 F1 would be useful.

Another possible interpretation of the results of the present study is that CA-AhR does not behave the same as ligand-bound AhR in the suppression of the GVH response. AhR-dependent changes in expression of genes, particularly those involved in the activation and differentiation of T-cells, and also non-genomic effects of AhR are reported to depend on the interaction of AhR with other proteins, such as transcription factors, co-activators, and co-repressors (reviewed in Hankinson, 2005; Harper et al., 2006). The deletion in a part of the ligand/Hsp90-binding site in the PAS B domain of AhR may affect the interaction of the CA-AhR with these other proteins and their function. In addition, it is possible that different ligands induce different conformational states, allowing for different protein interactions (Henry and Gasiewicz, 2003; Hestermann and Brown, 2003; Zhang et al., 2008). Recent studies have reported that activation of AhR by TCDD induces Treg, while activation of AhR by 6-formylindolo-[3,2-b]carbazole (FICZ) induces Th17 cells (Quintana et al., 2008; Veldhoen et al., 2008). These findings may indicate ligand-dependent regulation of AhR function. In contrast, the single-conformation available for the CA-AhR may not allow for interaction with other proteins.

In summary, our findings suggest that either activation of AhR must occur in other cells in addition to T-cells in order to cause immunosuppression or that CA-AhR does not behave exactly the same as ligand (TCDD)-bound AhR in the GvH model. Additional studies in progress of functions of CA-AhR will provide insights into the genomic and non-genomic mechanisms of AhR function.

Acknowledgements

We would like to thank Linda Steppan for her excellent technical advice, Dr. David Shepherd for his critical review of the manuscript, and Michiyo Matsumoto for her outstanding secretarial assistance.

Declaration of interest: The authors report no conflicts of interest. The authors alone are responsible for the content and writing of the paper.

References

Arbones, M. L., Ord, D. C., Ley, K., Ratech, H., Maynard-Curry, C., Otten, G., Capon, D. J., and Tedder, T. F. 1994. Lymphocyte homing and leukocyte rolling and migration are impaired in L-selectin-deficient mice. *Immunity* 1:247-260.

Boverhof, D. R., Tam, E., Harney, A. S., Crawford, R. B., Kaminski, N. E., and Zacharewski, T. R. 2004. 2,3,7,8-Tetrachlorodibenzo-*p*-dioxin induces suppressor of cytokine signaling 2 in murine B-cells. *Mol. Pharmacol.* 66:1662-1670.

Bradley, L. M., Watson, S. R., and Swain, S. L. 1994. Entry of naive CD4 T-cells into peripheral lymph nodes requires L-selectin. *J. Exp. Med.* 180:2401-2406.

Denison, M. S., and Nagy, S. R. 2003. Activation of the aryl hydrocarbon receptor by structurally-diverse exogenous and endogenous chemicals. *Annu. Rev. Pharmacol. Toxicol.* 43:309-334.

Ding, Z., Issekutz, T. B., Downey, G. P., and Waddell, T. K. 2003. L-Selectin stimulation enhances functional expression of surface CXCR4 in lymphocytes: Implications for cellular activation during adhesion and migration. *Blood* 101:4245-4252.

Friedline, R. H., Wong, C. P., Steeber, D. A., Tedder, T. F., and Tisch, R. 2002. L-Selectin is not required for T-cell-mediated autoimmune diabetes. *J. Immunol.* 168:2659-2666.

Funatake, C. J., Dearstyne, E. A., Steppan, L. B., Shepherd, D. M., Spanjaard, E. S., Marshak-Rothstein, A., and Kerkvliet, N. I. 2004. Early consequences of 2,3,7,8-tetrachlorodibenzo-*p*-dioxin exposure on the activation and survival of antigen-specific T-cells. *Toxicol. Sci.* 82:129-142.

Funatake, C. J., Marshall, N. B., Steppan, L. B., Mourich, D. V., and Kerkvliet, N. I. 2005. Cutting edge: activation of the aryl hydrocarbon receptor by 2,3,7,8-tetrachlorodibenzo-*p*-dioxin generates a population of $CD4^+CD25^+$ cells with characteristics of regulatory T-cells. *J. Immunol.* 175:4184-4188.

Funatake, C. J., Marshall, N. B., and Kerkvliet, N. I. 2008. 2,3,7,8-Tetrachlorodibenzo-*p*-dioxin alters the differentiation of alloreactive $CD8^+$ T-cells toward a regulatory T-cell phenotype by a mechanism that is dependent on aryl hydrocarbon receptor in $CD4^+$ T-cells. *J. Immunotoxicol.* 5:81-91.

Galkina, E., Tanousis, K, Preece, G., Tolaini, M., Kioussis, D., Florey, O., Haskard, D. O., Tedder, T. F., and Ager, A. 2003. L-Selectin shedding does not regulate constitutive T-cell trafficking but controls the migration pathways of antigen-activated T-lymphocytes. *J. Exp. Med.* 198:1323-1335.

Giblin, P. A., Hwang, S. T., Katsumoto, T. R., and Rosen, S. D. 1997. Ligation of L-selectin on T-lymphocytes activates β1 integrins and promotes adhesion to fibronectin. *J. Immunol.* 159:3498-3507.

Hankinson, O. 2005. Role of co-activators in transcriptional activation by the aryl hydrocarbon receptor. *Arch. Biochem. Biophys.* 433:379-386.

Harper, P. A., Riddick, D. S., and Okey, A. B. 2006. Regulating the regulator: Factors that control levels and activity of the aryl hydrocarbon receptor. *Biochem. Pharmacol.* 72:267-279.

Henry, E. C., and Gasiewicz, T. A. 2003. Agonist but not antagonist ligands induce conformational change in the mouse aryl hydrocarbon receptor as detected by partial proteolysis. *Mol. Pharmacol.* 63:392-400.

Hestermann, E. V., and Brown, M. 2003. Agonist and chemopreventative ligands induce differential transcriptional cofactor recruitment by aryl hydrocarbon receptor. *Mol. Cell. Biol.* 23:7920-7925.

Holsapple, M. P., Snyder, N. K., Wood, S. C., and Morris, D. L. 1991. A review of 2,3,7,8-tetrachlorodibenzo-*p*-dioxin-induced changes in immunocompetence: 1991 update. *Toxicology* 69:219-255.

Inouye, K., Ito, T., Fujimaki, H., Takahashi, Y., Takemori, T., Pan, X., Tohyama, C., and Nohara, K. 2003. Suppressive effects of 2,3,7,8-tetrachlorodibenzo-*p*-dioxin (TCDD) on the high-affinity antibody response in C57BL/6 mice. *Toxicol. Sci.* 74:315-324.

Jeuken, A., Keser, B. J., Khan, E., Brouwer, A., Koeman, J., and Denison, M. S. 2003. Activation of the Ah receptor by extracts of dietary herbal supplements, vegetables, and fruits. *J. Agric. Food Chem.* 51:5478-5487.

Kerkvliet, N. I. 2002. Recent advances in understanding the mechanisms of TCDD immunotoxicity. *Int. Immunopharmacol.* 2:277-291.

Kerkvliet, N. I. 2003. Immunotoxicology of dioxins and related chemicals. In: *Dioxins and Health*, 2nd Edition (Schecter, A., and Gasiewicz, T. A., Eds.), New York: John Wiley & Sons, Inc., pp. 299-328.

Kerkvliet, N. I., Shepherd, D. M., and Baecher-Steppan, L. 2002. T-Lymphocytes are direct, aryl hydrocarbon receptor (AhR)-dependent targets of 2,3,7,8-tetrachlorodibenzo-*p*-dioxin (TCDD): AhR expression in both $CD4^+$ and $CD8^+$ T-cells is necessary for full suppression of a cytotoxic T-lymphocyte response by TCDD. *Toxicol. Appl. Pharmacol.* 185:146-152.

Kimura, A., Naka, T., Nohara, K., Fujii-Kuriyama, Y., and T., Kishimoto. 2008. Aryl hydrocarbon receptor regulates Stat1 activation and participates in the development of Th17 cells. *Proc. Natl. Acad. Sci. USA* 105:9721-9726.

Laiosa, M. D., Wyman, A., Murante, F. G., Fiore, N. C., Staples, J. E., Gasiewicz, T. A., and Silverstone, A. E. 2003. Cell proliferation arrest within intrathymic lymphocyte progenitor cells causes thymic atrophy mediated by the aryl hydrocarbon receptor. *J. Immunol.* 171:4582-4591.

Lawrence, B. P., and Kerkvliet, N. I. 2007. Immune modulation by TCDD and related polyhalogenated aromatic hydrocarbons. In: *Immunotoxicology and Immunopharmacology*, 3rd Edition (Luebke, R., House, R., and I., Kimber, I., Eds.), Boca Raton, FL: Taylor & Francis, pp. 239-258.

Lawrence, B. P., Roberts, A. D., Neumiller, J. J., Cundiff, J. A., and Woodland, D. L. 2006. Aryl hydrocarbon receptor activation impairs the priming but

not the recall of influenza virus-specific CD8⁺ T-cells in the lung. *J. Immunol.* 177:5819-5828.

Liem, A. K., Furst. P., and Rappe. C. 2000. Exposure of populations to dioxins and related compounds. *Food Addit. Contam.* 17:241-259.

McGuire, J., Okamoto, K., Whitelaw, M. L., Tanaka, H., and Poellinger, L. 2001. Definition of a dioxin receptor mutant that is a constitutive activator of transcription: Delineation of overlapping repression and ligand binding functions within the PAS domain. *J. Biol. Chem.* 276:41841-41849.

Mimura, J., and Fujii-Kuriyama, Y. 2003. Functional role of AhR in the expression of toxic effects by TCDD. *Biochem. Biophys. Acta* 1619:263-268.

Moennikes, O., Loeppen, S., Buchmann, A., Andersson, P., Ittrich, C., Poellinger, L., and Schwarz, M. 2004. A constitutively-active dioxin/aryl hydrocarbon receptor promotes hepatocarcinogenesis in mice. *Cancer Res.* 64:4707-4710.

Mora, C., Grewal, I. S., Wong, F. S., and Flavell, R. A. 2004. Role of L-selectin in the development of autoimmune diabetes in non-obese diabetic mice. *Int. Immunol.* 16:257-264.

Nguyen, L. P., and Bradfield, C. A. 2008. The search for endogenous activators of the aryl hydrocarbon receptor. *Chem. Res. Toxicol.* 21:102-116.

Nohara, K., Fujimaki, H., Tsukumo, S., Inouye, K., Sone, H., and Tohyama, C. 2002. Effects of 2,3,7,8-tetrachlorodibenzo-*p*-dioxin (TCDD) on T-cell-derived cytokine production in ovalbumin (OVA)-immunized C57Bl/6 mice. *Toxicology* 172:49-58.

Nohara, K., Pan, X., Tsukumo, S., Hida, A., Ito, T., Nagai, H., Inouye, K., Motohashi, H., Yamamoto, M., Fujii-Kuriyama, Y., and Tohyama, C. 2005. Constitutively active aryl hydrocarbon receptor expressed specifically in T-lineage cells causes thymus involution and suppresses the immunization-induced increase in splenocytes. *J. Immunol.* 174:2770-2777.

Nohara, K., Suzuki, T., Ao, K., Murai, H., Miyamoto, Y., Inouye, K., Pan, X., Motohashi, H., Fujii-Kuriyama, Y., Yamamoto, M., and Tohyama, C. 2009. Constitutively active aryl hydrocarbon receptor expressed in T-cells increases immunization-induced IFNγ production in mice but does not suppress T_H2-cytokine production or antibody production *Int. Immunology.* 21:769-777.

Quintana, F. J., Basso, A. S., Iglesias, A. H., Korn, T., Farez, M. F., Bettelli, E., Caccamo, M., Oukka, M., and Weiner, H. L. 2008. Control of T(reg) and T(H)17 cell differentiation by the aryl hydrocarbon receptor. *Nature* 453:65-71.

Ruby, C. E., Funatake, C. J., and Kerkvliet, N. I. 2005. 2,3,7,8-Tetrachlorodibenzo-*p*-dioxin (TCDD) directly enhances the maturation and apoptosis of dendritic cells *in vitro*. *J. Immunotoxicol.* 1:159-166.

Schecter, A., Cramer, P., Boggess, K., Stanley, J., Papke, O., Olson, J., Silver, A., and Schmitz, M. 2001. Intake of dioxins and related compounds from food in the U.S. population. *J. Toxicol. Environ. Health A* 63:1-18.

Schmidt, J. V., and Bradfield, C. A. 1996. Ah receptor signaling pathways. *Annu. Rev. Cell Dev. Biol.* 12:55-89.

Schmidt, J. V., Su, G. H., Reddy, J. K., Simon, M. C., and Bradfield, C. A. 1996. Characterization of a murine Ahr null allele: Involvement of the Ah receptor in hepatic growth and development. *Proc. Natl. Acad. Sci. USA* 93:6731-6736.

Shepherd, D. M., Dearstyne, E. A., and Kerkvliet, N. I. 2000. The effects of TCDD on the activation of ovalbumin (OVA)-specific DO11.10 transgenic CD4⁺ T-cells in adoptively transferred mice. *Toxicol. Sci.* 56:340-350.

Startin, J. R., and Rose, M. D. 2003. Dioxins and dioxin-like PCBs in food. In: *Dioxins and Health*, 2nd Edition (Schecter, A., and Gasiewicz, T. A., Eds.), New York: John Wiley & Sons, Inc., pp. 89-136.

Sulentic, C. E. W., Holsapple, M. P., and Kaminski, N. E. 1998. Aryl hydrocarbon receptor-dependent suppression by 2,3,7,8-tetrachlorodibenzo-*p*-dioxin of IgM secretion in activated B-cells. *Mol. Pharmacol.* 53:623-629.

Sun, Y. V., Boverhof, D. R., Burgoon, L. D., Fielden, M. R., and Zacharewski, T. R. 2004. Comparative analysis of dioxin response elements in human, mouse and rat genomic sequences. *Nucl. Acids Res.* 32:4512-4523.

Veldhoen, M., Hirota, K., Westendorf, A. M., Buer, J., Dumoutier, L., Renauld, J. C., and Stockinger, B. 2008. The aryl hydrocarbon receptor links TH17-cell-mediated autoimmunity to environmental toxins. *Nature* 453:106-109.

Vorderstrasse, B. A., and Kerkvliet, N. I. 2001. 2,3,7,8-Tetrachlorodibenzo-*p*-dioxin affects the number and function of murine splenic dendritic cells and their expression of accessory molecules. *Toxicol. Appl. Pharmacol.* 171:117-125.

Vorderstrasse, B. A., Dearstyne, E. A., and Kerkvliet, N. I. 2003. Influence of 2,3,7,8-tetrachlorodibenzo-*p*-dioxin on the antigen-presenting activity of dendritic cells. *Toxicol. Sci.* 72:103-112.

Warnock, R. A., Askari, S., Butcher, E. C., and von Andrian, U. H. 1998. Molecular mechanisms of lymphocyte homing to peripheral lymph nodes. *J. Exp. Med.* 187:205-216.

Zhang, S., Rowlands, C., and Safe, S. 2008. Ligand-dependent interactions of the Ah receptor with co-activators in a mammalian two-hybrid assay. *Toxicol. Appl. Pharmacol.* 227:196-206.

EMBO reports

scientific report

G-protein signalling negatively regulates the stability of aryl hydrocarbon receptor

Asuka Nakata[1], Daisuke Urano[1], Yoshiaki Fujii-Kuriyama[2], Norikazu Mizuno[1], Kenji Tago[1+] & Hiroshi Itoh[1]

[1]Department of Cell Biology, Graduate School of Biological Sciences, Nara Institute of Science and Technology, Takayama, Ikoma, Nara, Japan, and [2]Center for Tsukuba Advanced Research Alliance and Institute of Basic Medical Sciences, University of Tsukuba, Tsukuba, Ibaraki, Japan

Aryl hydrocarbon receptor (AhR) is a transcription factor that works as a dioxin receptor and is also involved in various physiological phenomena, including development and cell proliferation. Here, we show that the $G\alpha_{13}$ signal destabilizes AhR by promoting the ubiquitination of AhR. $G\alpha_{13}$ interacts directly with AhR-interacting protein (AIP) and inhibits the interaction between AhR and AIP, a crucial interacting protein of AhR. Strikingly, a reporter gene assay and a quantitative reverse transcription–PCR analysis indicate that the $G\alpha_{13}$ signal shows a potent inhibitory effect on the ligand-induced transcriptional activation of AhR. $G\alpha_{13}$ results in the nuclear translocation of AhR in a ligand-independent manner. However, in the presence of active $G\alpha_{13}$, AhR fails to form the active transcriptional complex. Taken together, we propose a new negative regulation of dioxin signalling by the G protein.

Keywords: dioxin receptor; G protein; ubiquitin

EMBO reports (2009) 10, 622–628. doi:10.1038/embor.2009.35

INTRODUCTION

Aryl hydrocarbon receptor (AhR) is a ligand-activated transcription factor that belongs to the bHLH-PAS (basic helix–loop–helix PER/Arnt/Sim) superfamily (Schmidt & Bradfield, 1996; Mimura & Fujii-Kuriyama, 2003). AhR is broadly expressed in various tissues and is involved both in diverse responses to dioxin and in female reproduction by regulating the expression of aromatase in ovarian cells (Baba *et al*, 2005).

In the absence of stimulation, AhR is localized in the cytoplasm and associates with two molecules of the molecular chaperone heat-shock protein 90 (HSP90), the co-chaperone p23 and the immunophilin-like protein AIP (AhR-interacting protein, also known as XAP2 or Ara9; Mimura & Fujii-Kuriyama, 2003). On ligand binding, AhR undergoes a conformational change and translocates into the nucleus. In the nucleus, AhR binds to Arnt and forms a transcriptionally active complex. AhR in the active complex binds to xenobiotic response element (XRE) in the promoter region of the target genes, which include many drug-metabolizing enzymes, such as P450/CYP1A (Fujii-Kuriyama & Mimura, 2005). At present, the endogenous ligand for AhR remains unknown; however, the transcriptional activity of AhR can be stimulated by various xenobiotic compounds, including 2,3,7,8-TCDD (2,3,7,8-tetrachlorodibenzo-*p*-dioxin) and 3-MC (3-methyl cholanthrene).

AIP facilitates the activation of AhR and contributes to the maintenance of AhR in the cytoplasm. The amino-terminal part of AIP contains regions that have homology with FK506-binding protein 12 (FKBP12) and FKBP52, but AIP does not bind to FK506 (Fig 1A). The carboxy-terminal part of AIP contains three TPR (tetratricopeptide repeat) motifs, which are involved in protein–protein interactions. AIP protects AhR from ubiquitination, resulting in stabilization (Kazlauskas *et al*, 2000; LaPres *et al*, 2000). AIP also regulates the subcellular localization of AhR, indicating that AIP is crucial in AhR signalling. It has been reported that AIP binds to other nuclear receptors, including peroxisome proliferator-activated receptor-α and thyroid hormone receptor-β1, and affects their transcriptional activity (Sumanasekera *et al*, 2003; Froidevaux *et al*, 2006). These reports indicate that AIP takes part in various nuclear receptor signalling pathways.

Heterotrimeric G proteins are composed of three subunits, α, β and γ (Gα, Gβ and Gγ), and function as molecular switches that turn on intracellular signalling cascades in response to the activation of G-protein-coupled receptors (GPCRs) by extracellular stimulation including sensory signals, hormones, neurotransmitters and chemokines in mammalian cells (Gilman, 1987; Kaziro *et al*, 1991). G proteins are typically characterized into four main classes on the basis of the primary sequence similarity of the Gα-subunits: G_s, G_i, G_q and G_{12}. Among them, the two members of the G_{12} family, G_{12} and G_{13}, have been reported to interact directly with p115RhoGEF, Na^+-H^+ exchanger, radixin, cadherin and protein phosphatase 5 (Kurose, 2003). The α-subunits of G_{12}

[1]Department of Cell Biology, Graduate School of Biological Sciences, Nara Institute of Science and Technology, 8916-5 Takayama, Ikoma, Nara 630-0192, Japan
[2]Center for Tsukuba Advanced Research Alliance and Institute of Basic Medical Sciences, University of Tsukuba, 1-1-1 Tennodai, Tsukuba, Ibaraki 305-8577, Japan
+Corresponding author. Tel: +81 743 72 5444; Fax: +81 743 72 5449;
E-mail: ktago@bs.naist.jp

Received 23 September 2008; revised 22 January 2009; accepted 12 February 2009; published online 24 April 2009

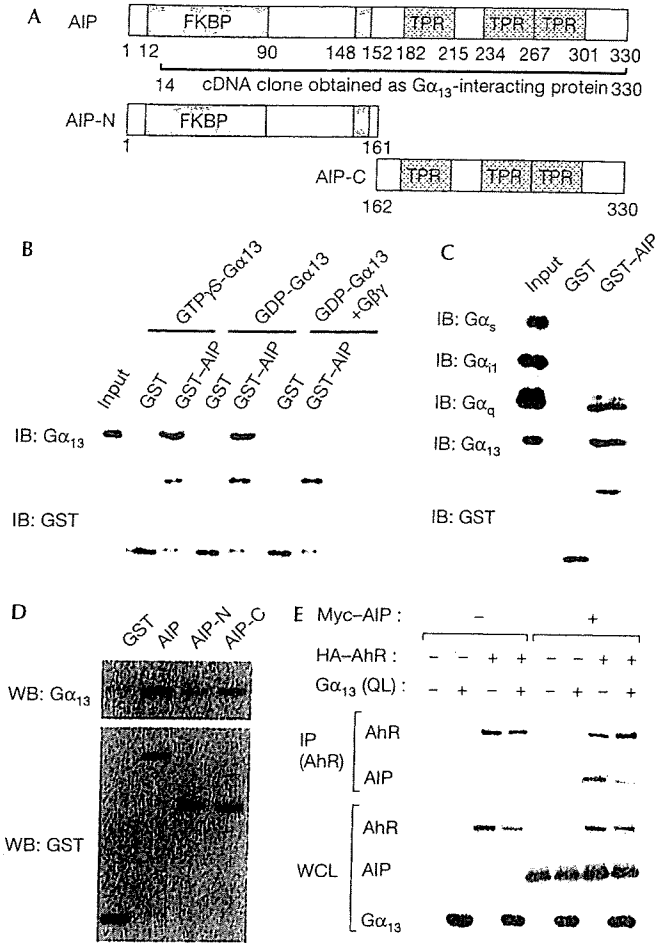

Fig 1 | AIP is identified as a $G\alpha_{13}$-interacting protein. (A) AIP contains the FKBP domain and three TPR motifs. The AIP fragment shown was isolated by a yeast two-hybrid screen. The amino- and carboxy-terminal fragments of AIP used in subsequent experiments are also shown. (B) Recombinant $G\alpha_{13}$ was treated with 10 μM GTPγS, 100 μM GDP or GDP plus Gβγ, and then mixed with GST or GST–AIP. The interaction between $G\alpha_{13}$ and AIP was detected by immunoblot (IB). (C,D) The interaction between a series of Gα subunits and GST–AIP or its mutants (illustrated in (A)) was analysed by the same procedures as in (B). (E) The whole-cell lysate (WCL) of HEK293T cells transfected as indicated was used for immunoprecipitation with the HA antibody. Experiments were performed three times, and similar results were observed. AIP, AhR-interacting protein; FKBP, FK506-binding protein; GST, glutathione *S*-transferase; HA, haemagglutinin; HEK, human embryonic kidney; TPR, tetratricopeptide repeat.

and G_{13} ($G\alpha_{12}$ and $G\alpha_{13}$) are ubiquitously expressed and coupled to the receptors, which respond to lysophosphatidic acid (LPA), sphingosine 1-phosphate (S1P) and thrombin. Although the primary structure of $G\alpha_{12}$ and $G\alpha_{13}$ shows 67% similarity, the physiological roles of $G\alpha_{12}$ and $G\alpha_{13}$ seem to be different, as only $G\alpha_{13}$-deficient mice show the embryonic lethal phenotype and $G\alpha_{12}$-deficient mice do not.

In the course of our study to identify the new downstream effectors of $G\alpha_{13}$, we found that $G\alpha_{13}$ signalling represses AhR-mediated transcription by affecting the localization and stability of AhR. We propose the new concept that AhR is negatively regulated by G-protein signalling.

RESULTS AND DISCUSSION

$G\alpha_{13}$ interacts with AIP

To identify new $G\alpha_{13}$-interacting proteins, we performed a yeast two-hybrid screen by using $G\alpha_{13}$Q226L, a mutant lacking GTPase activity, as bait. From the mouse fetal brain cDNA library, we obtained two clones, both of which encoded AIP (Fig 1A). To confirm the interaction between $G\alpha_{13}$ and AIP, we prepared recombinant proteins and then performed *in vitro* pull-down analysis. As shown in Fig 1B, we observed that both the GDP and GTP forms of $G\alpha_{13}$ interacted comparably with AIP, suggesting that the interaction between $G\alpha_{13}$ and AIP is independent of GDP/GTP-binding status. Next, we tested the effect of the Gβγ-subunit on the association between $G\alpha_{13}$ and AIP. The addition of Gβγ effectively abolished the interaction between $G\alpha_{13}$ and AIP, suggesting that the dissociation of $G\alpha_{13}$ from Gβγ seems to be required for the formation of the $G\alpha_{13}$–AIP complex. Also, we tested the ability of other Gα-subunits—$G\alpha_s$, $G\alpha_{i1}$ and $G\alpha_q$—to interact with AIP. As shown in Fig 1C, $G\alpha_q$ showed less binding than did $G\alpha_{13}$; however, $G\alpha_s$ and $G\alpha_{i1}$ failed to bind to AIP. As shown in Fig 1A, the C-terminus of AIP contains three TPR motifs, which are involved in protein–protein interactions (Blatch & Lässle, 1999). Some proteins containing TPR motifs, such as protein phosphatase 5 and TPR1, interact with heterotrimeric G protein through their TPR motifs (Yamaguchi *et al*, 2002; Marty *et al*, 2003). To determine the region of AIP that binds to $G\alpha_{13}$, we prepared deletion mutants of AIP and used them for an *in vitro* binding assay. As shown in Fig 1D, $G\alpha_{13}$ could interact with both the N- and C-terminal portions of AIP. It has been reported that the TPR motifs of AIP are involved in the association of AIP and AhR (Meyer *et al*, 2000), and that $G\alpha_{13}$ also showed the ability to bind to the C terminus of AIP, suggesting that $G\alpha_{13}$ might physically disturb the interaction of AhR with AIP by competition of the TPR motifs of AIP. We tested whether $G\alpha_{13}$ counteracts the complex formation of AIP with AhR. Using human embryonic kidney 293T (HEK293T) cells expressing AIP, AhR and/or $G\alpha_{13}$Q226L, immunoprecipitation analysis was performed. As reported previously (Carver & Bradfield, 1997), AIP interacted with AhR. However, the coexpression of $G\alpha_{13}$Q226L suppressed the interaction between AIP and AhR (Fig 1E). AIP has been reported to form a complex with AhR and HSP90 in the cytoplasm, and this complex formation is necessary for the ligand-mediated activation of AhR (Meyer *et al*, 1998). Our data raise the interesting possibility that $G\alpha_{13}$ might affect the ligand-mediated activation of AhR.

Activation of $G\alpha_{13}$ inhibits AhR-mediated transcription

To examine whether $G\alpha_{13}$ affects the ligand-dependent activation of AhR, we performed an XRE-driven luciferase reporter gene assay. When AhR and AIP were exogenously expressed in COS-7 cells, 3-MC induced the AhR-dependent activation of XRE, as shown in Fig 2A. Interestingly, the expression of $G\alpha_{13}$Q226L effectively suppressed the 3-MC-induced XRE activation. Next, we examined whether a small GTP-binding protein, Rho, is involved in the inhibition of AhR by $G\alpha_{13}$, as $G\alpha_{13}$ induces the activation of Rho through p115RhoGEF. An active mutant of RhoA, RhoA(G14V), failed to affect the 3-MC-induced luciferase activity

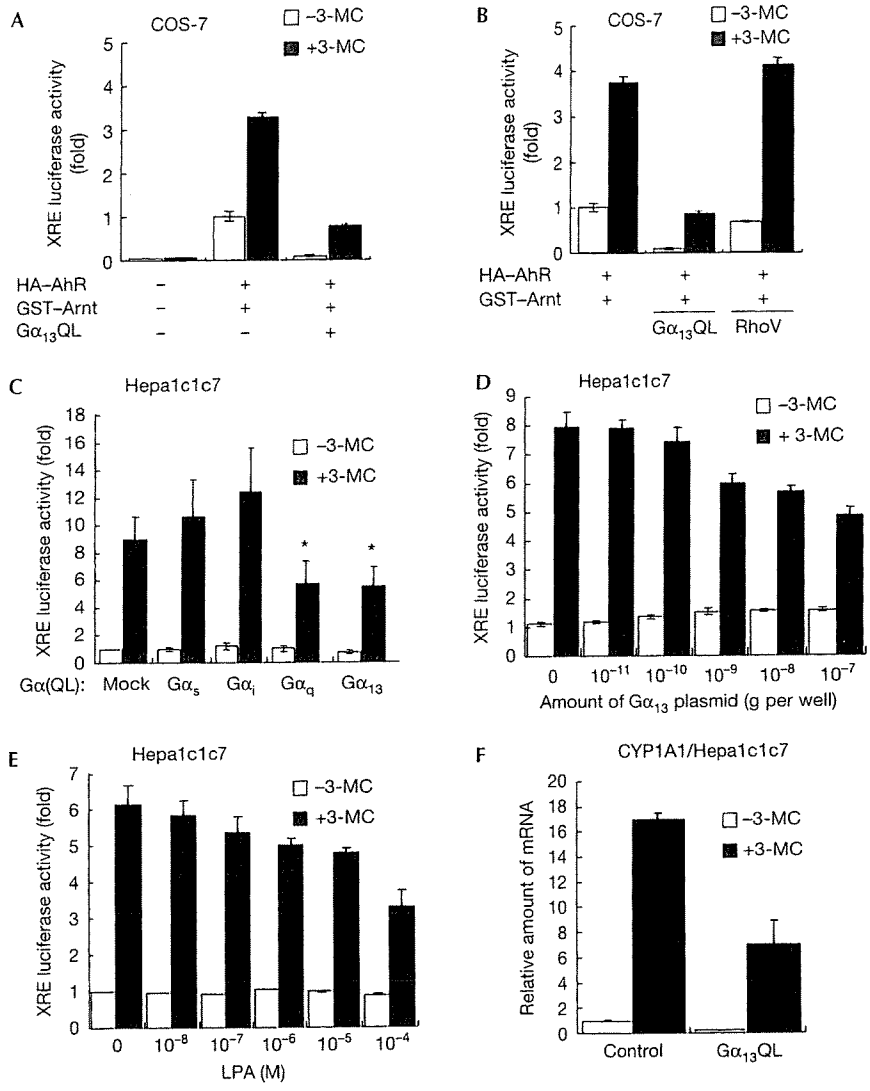

Fig 2 | Activated $G\alpha_{13}$ inhibits AhR-mediated transcriptional activity. (**A**,**B**) COS-7 cells transfected as indicated were stimulated with 1 μM 3-MC and then used for the luciferase reporter gene analysis. (**C**,**D**) Hepa1c1c7 cells expressing constitutively active mutants of Gα were stimulated with or without 1 μM 3-MC for 24 h, and then the luciferase reporter gene analysis was performed. In (**D**), Hepa1c1c7 cells were transfected with various amounts of $G\alpha_{13}$Q226L. (**E**) Hepa1c1c7 cells harbouring a reporter gene were pretreated with various concentrations of LPA, and were then stimulated with 3-MC and used for reporter gene analysis. (**F**) Hepa1c1c7 cells transfected with or without $G\alpha_{13}$Q226L were treated with 1 μM 3-MC for 12 h. The expression of CYP1A1 was analysed by the quantitative RT–PCR method. Error bar means s.e. ($n = 3$, $^*P < 0.05$). 3-MC, 3-methyl cholanthrene; AhR, aryl hydrocarbon receptor; GST, glutathione *S*-transferase; HA, haemagglutinin; LPA, lysophosphatidic acid; RT–PCR, reverse transcription–PCR.

(Fig 2B). These data suggest that the active $G\alpha_{13}$ inhibits the activation of AhR in a RhoA-independent manner. Next, we tested the effect of various Gα-subunits on endogenous activation of AhR using Hepa1c1c7 cells, which express highly the endogenous AhR and AIP. As shown in Fig 2C, $G\alpha_{13}$Q226L and $G\alpha_q$Q209L inhibited the XRE-driven luciferase activity and $G\alpha_{13}$Q226L showed the dose-dependent inhibition of AhR (Fig 2D). The Gα specificity of suppression of luciferase activity was correlated with the ability of Gα to bind to AIP (Figs 1C,2C), implying that the interaction of Gα with AIP could trigger the suppression of AhR. LPA is known to activate $G\alpha_{13}$ through its receptor. Stimulation by LPA also suppressed 3-MC-induced activation of AhR in a dose-dependent manner (Fig 2E), indicating that the physiological activation of the $G\alpha_{13}$ signal suppresses the activation of AhR. Next, we investigated the effect of $G\alpha_{13}$ on AhR-induced CYP1A1 expression using quantitative reverse transcription–PCR (RT–PCR) analysis. In Hepa1c1c7 cells, 3-MC induced the expression of CYP1A1, and this induction was markedly decreased when $G\alpha_{13}$Q226L was expressed (Fig 2F). These data suggest that the activation of $G\alpha_{13}$ inhibits the AhR-mediated transcriptional activity.

The localization of AhR is altered by $G\alpha_{13}$

AhR is a nucleocytoplasmic shuttling protein, and AIP is crucial in the cytoplasmic localization of AhR (Petrulis *et al*, 2003). To examine the effect of $G\alpha_{13}$ on the localization of AhR, we

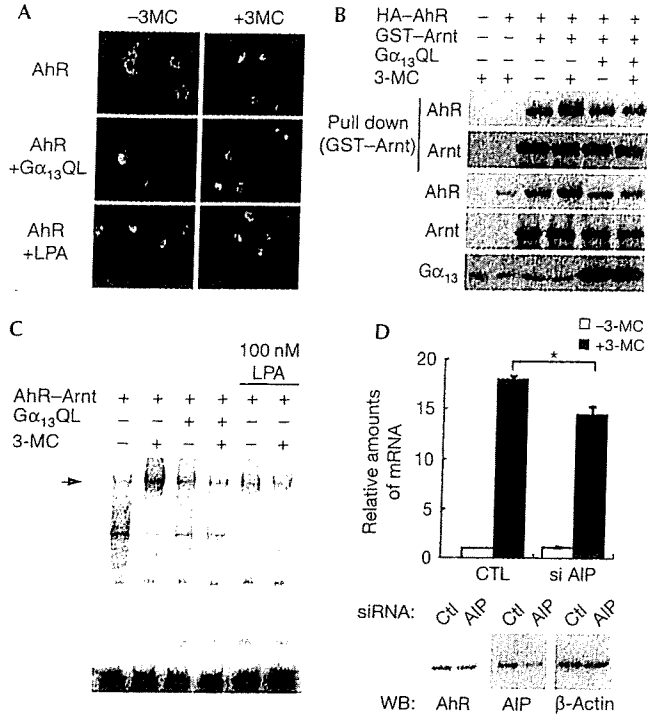

Fig 3 | The subcellular localization, dimerization with Arnt and DNA-binding activity of AhR are altered by the activation of $G\alpha_{13}$. (A) COS-7 cells expressing HA–AhR, GST–Arnt or $G\alpha_{13}$Q226L were stimulated with 3-MC and/or LPA for 24 h. The localization of AhR was visualized by immunostaining with the HA antibody. (B) COS-7 cells transfected as indicated were stimulated with 1 μM 3-MC for 6 h. The protein complexes were precipitated and analysed by immunoblot analysis. (C) COS-7 cells transfected with the indicated combinations of plasmids were stimulated with 1 μM 3-MC for 6 h. Nuclear extracts were analysed by EMSA with the radioactively labelled AhR-binding element DNA probe. An arrow indicates the AhR–Arnt complex binding to the probe. (D) Hepa1c1c7 cells were transfected with the indicated siRNA mixture, and stimulated with 1 μM 3-MC for 12 h. The expression of CYP1A1 was analysed by the quantitative RT-PCR method. Expression of AhR, AIP and β-actin were analysed by immunoblot. 3-MC, 3-methyl cholanthrene; AhR, aryl hydrocarbon receptor; AIP, AhR-interacting protein; Ctl, control; EMSA, electrophoretic mobility shift assay; GST, glutathione *S*-transferase; HA, haemagglutinin; LPA, lysophosphatidic acid; RT–PCR, reverse transcription–PCR; siRNA, short interfering RNA.

examined by using immunofluorescence analysis where AhR localizes under the activation of $G\alpha_{13}$. Haemagglutinin-tagged AhR expressed in COS-7 cells was observed in the cytoplasm in quiescent cells. Once cells were stimulated by 3-MC, AhR translocated to the nucleus (Fig 3A). Interestingly, the expression of $G\alpha_{13}$Q226L and LPA stimulation resulted in the nuclear translocation of AhR despite the absence of 3-MC (Fig 3A). It is known that an interaction between AhR and AIP is required for the localization of AhR in the cytoplasm, as well as for the ligand-mediated transcriptional activation of AhR (Meyer *et al*, 1998). As $G\alpha_{13}$ inhibited the association of AhR with AIP (Fig 1E), the $G\alpha_{13}$-induced dissociation of AhR from AIP might lead to the translocation of AhR to the nucleus. Although 3-MC induced the translocation of AhR to the nucleus followed by the transactivation of AhR, the nuclear localization of AhR induced by $G\alpha_{13}$ failed to induce the transactivation of AhR (Fig 2). To investigate whether nuclear-accumulated AhR by $G\alpha_{13}$ is not in an 'active state', we examined the effect of $G\alpha_{13}$ on the ability of AhR to interact with Arnt. We introduced GST–Arnt and AhR with or without $G\alpha_{13}$Q226L into COS-7 cells, and then GST pull-down analysis was performed to detect the AhR/GST–Arnt protein complex. As shown in Fig 3B, the stimulation with 3-MC enhanced the complex formation of Arnt and AhR (Fig 3B, lanes 3 and 4). Interestingly, the expression of $G\alpha_{13}$Q226L prevented the 3-MC-induced complex formation of Arnt and AhR (Fig 3B, lanes 5 and 6). This result suggests that AhR accumulated in the nucleus by $G\alpha_{13}$ is not in an active complex. To verify this hypothesis, we next tested by using an electrophoretic mobility shift assay (EMSA) whether the $G\alpha_{13}$ signal affects the binding activity of AhR to XRE. When AhR and Arnt were ectopically expressed in COS-7 cells, the nuclear extract from the cells treated with 3-MC showed binding activity to a DNA probe including XRE (supplementary Fig 1 online). The expression of $G\alpha_{13}$Q226L prevented the 3-MC-induced DNA-binding activity of AhR (Fig 3C). LPA also inhibited the formation of the AhR–DNA complex. It is well established that the transcriptional activation of AhR requires a ligand-induced conformational change that confers the ability of nuclear translocation and heterodimer formation of AhR with Arnt. This heterodimer formation leads to their binding to an XRE element. By contrast, our results indicated that $G\alpha_{13}$ induces the nuclear accumulation of AhR without ligand stimulation. However, in the presence of the $G\alpha_{13}$ signal, AhR showed no ability to form the complex with Arnt and failed to bind to XRE, because of lacking the conformational change of AhR. Next, to test whether sequestering AIP from the AhR complex is enough for the $G\alpha_{13}$-induced suppressive effect on the activation of AhR, we used RNA interference to knock down AIP. The activation of AhR was partly reduced by small interfering RNA (siRNA) of AIP but could still be activated by 3-MC stimulation (Fig 3D). In addition, we fractionated the cytoplasm and nucleus from Hepa1c1c7 cells and analysed the localization of AhR. As shown in supplementary Fig 2 online, knockdown of AIP showed a fairly weak effect on AhR localization in the nucleus without 3-MC. The knockdown of AIP did not fully mimic the effect of $G\alpha_{13}$ on the AhR signal, indicating that $G\alpha_{13}$ not only disturbed the association between AhR and AIP but also affected other signals to suppress the activation of AhR. Lees & Whitelaw (2002) reported that antisense oligonucleotide for AIP decreased the activation of AhR in HEK293T cells. Conversely, it has also been reported that knockdown of AIP failed to shut down ligand-induced activation of AhR (Pollenz & Dougherty, 2005). Our current result seems to fall somewhere inbetween these two reports, and we have no additional information to explain this discrepancy. However, a study using an animal experiment showed that AIP is essential for AhR signalling (Lin *et al*, 2008). Clarification of the physiological role of AIP is a problem that needs to be explored.

$G\alpha_{13}$ promotes the destabilization of AhR

As described in the Introduction, in quiescent cells, AIP forms a stable complex with AhR and protects it from degradation by the ubiquitin–proteasome pathway. We observed that $G\alpha_{13}$

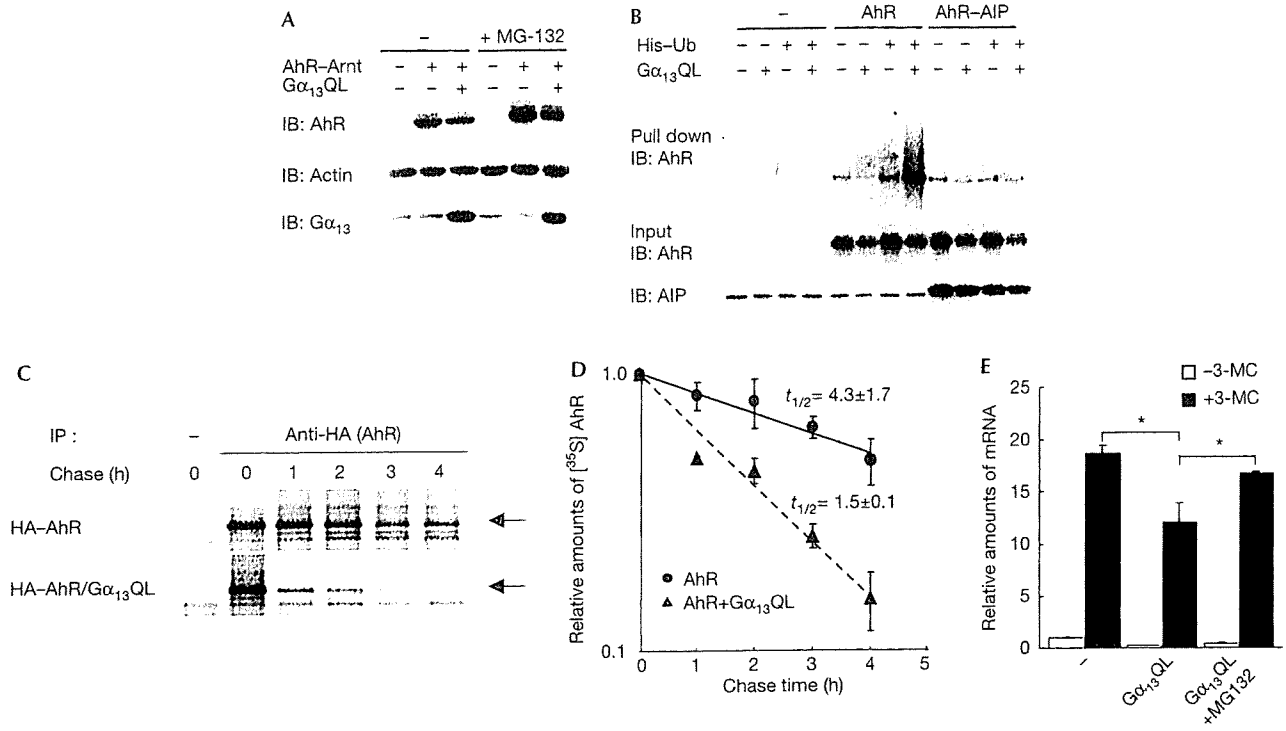

Fig 4 | $G\alpha_{13}$ induces the ubiquitination and degradation of AhR. (**A**) HEK293T cells transfected as indicated were treated with or without 10 μM MG-132 for 4 h. Then, cell lysates were analysed by immunoblot (IB) analysis with the indicated antibodies. (**B**) HEK293T cells expressing $[His]_6$-ubiquitin (Ub), HA-AhR and Myc-AIP with or without $G\alpha_{13}Q226L$ were lysed, and the ubiquitinated proteins were precipitated by Ni-NTA agarose. The ubiquitinated AhR, AhR and AIP in the total lysate were analysed by immunoblot. (**C**,**D**) HEK293T cells transfected as indicated were tagged metabolically with [^{35}S]-labelled methionine and cysteine for 1 h. Then, the cells were used for pulse-chase analysis. The values of $t_{1/2}$ were obtained from three independent experiments. Arrows indicate immunoprecipitated AhR. (**E**) Hepa1c1c7 cells were transfected as indicated and stimulated with 1 μM 3-MC for 8 h in the presence or absence of 10 μM MG-132. The expression of CYP1A1 was analysed by the quantitative RT-PCR method. 3-MC, 3-methyl cholanthrene; AhR, aryl hydrocarbon receptor; AIP, AhR-interacting protein; HA, haemagglutinin; HEK, human embryonic kidney.

overexpression disturbed the association of AIP with AhR, suggesting that $G\alpha_{13}$ might impede the stabilization of AhR by AIP. We confirmed that the overexpression of $G\alpha_{13}Q226L$ resulted in the downregulation of the AhR protein (Fig 4A, lanes 2 and 3) and that the proteasome inhibitor, MG-132, restored the downregulation of AhR (Fig 4A, lanes 5 and 6). Then, we tested the effect of $G\alpha_{13}$ on the ubiquitination of AhR. HEK293T cells were transfected with AhR and histidine-tagged ubiquitin. Ubiquitinated AhR was precipitated by Ni-agarose and detected by immunoblot. As expected, the ubiquitination of AhR was promoted by $G\alpha_{13}Q226L$ (Fig 4B, lanes 7 and 8). Conversely, the ubiquitination of AhR was suppressed by the overexpression of AIP (Fig 4B, lanes 9–12). Next, to examine whether $G\alpha_{13}$ affects the protein stability of AhR, pulse-chase analysis was performed. The half-life of AhR was about 4.3 h in the absence of $G\alpha_{13}Q226L$. Conversely, when $G\alpha_{13}Q226L$ was coexpressed, AhR was degraded with a half-life of 1.5 h (Fig 4C,D). These data suggest that $G\alpha_{13}$ suppresses the activation of AhR through the destabilization of AhR by the ubiquitin–proteasome pathway. This possibility was also supported by the evidence that the expression of AhR was reduced by $G\alpha_{13}$ expression (Figs 1E,3B,4B). Interestingly, as shown in Fig 1E, overexpression of AIP effectively cancelled the $G\alpha_{13}$-induced reduction of AhR in whole-cell lysate (compare lanes 3 and 4, with lanes 7 and 8), and also in Fig 4B, coexpressed AIP diminished the ubiquitination of AhR accelerated by $G\alpha_{13}$. These results supported our hypothesis that $G\alpha_{13}$ competitively sequesters AIP from the AhR complex and this would be the trigger for $G\alpha_{13}$-induced suppression of activation of AhR. Also, we tested whether inhibition of proteasome is able to cancel the $G\alpha_{13}$-induced suppression of activation of AhR. As shown in Fig 4E, a proteasome inhibitor MG-132 showed the cancellation of the inhibitory effect of $G\alpha_{13}$, suggesting that promoting the proteasome-mediated degradation of AhR is one of the molecular mechanisms by which $G\alpha_{13}$ diminishes ligand-dependent activation of AhR. As shown in Fig 3, $G\alpha_{13}$ induced the ligand-independent nuclear localization of AhR, but did not allow AhR to interact with Arnt. It has been reported that the nuclear-localized AhR is unstable and degraded more rapidly in the absence of Arnt (Roberts & Whitelaw, 1999). This report supports our model that the $G\alpha_{13}$-induced nuclear localization of AhR might be the trigger for the degradation of AhR.

Through our current research, we have also shown that G_q has a potent inhibitory effect on AhR in spite of its weak interacting activity. Several signalling molecules have been reported to regulate the AhR signal. Some of them are activated by

$G\alpha_q$ signalling, including the transcription factor NF-κB (Harper *et al*, 2006). $G\alpha_q$ might affect AhR through these downstream molecules.

The C terminus of HSC70-interacting protein (CHIP) is known as E3 ligase, which contains three TPR motifs and a U-box domain (McDonough & Patterson, 2003), and has been reported to be involved in the ubiquitination of AhR (Lees *et al*, 2003). CHIP might be E3 ubiquitin ligase in the $G\alpha_{13}$-induced degradation of AhR. Here, we propose a new model to explain how the activation of AhR is attenuated by extracellular signals. The determination of which E3 ubiquitin ligase is involved in the $G\alpha_{13}$-induced suppression of AhR activity should be the focus of a future study.

METHODS

Cell culture and transfection. HEK293T, COS-7 and Hepa1c1c7 cells were maintained in Dulbecco's modified Eagle's medium supplemented with 10% FBS and 100 μg/ml kanamycin at 37 °C and 5% CO_2. Transfection into HEK293T and COS-7 cells was performed using the calcium phosphate method. Hepa1c1c7 cells were transfected using Lipofectamine2000 (Invitrogen; Carlsbad, CA, USA).

RNA interference. Annealed siRNA complexes for mouse AIP and firefly luciferase were purchased from Thermo Fisher Scientific Inc. (Waltham, MA, USA). The mixture of siRNA (final concentration, 50 nM) was transfected by using Lipofectamine2000 into 35-mm dishes containing 1×10^5 Hepa1c1c7 cells. At 48 h after transfection, cells were analysed as described in the text. The sequences of siRNA were shown in supplementary Fig 2A online.

Reporter gene analysis. For reporter gene analysis, cells were plated onto a 48-well plate. COS-7 or Hepa1c1c7 cells transfected with the indicated combinations of plasmids, including haemagglutinin–AhR, GST–Arnt, FLAG–$G\alpha_{13}$Q226L, pXRE–luciferase and pEF–RL, were stimulated with 1 μM 3-MC or 10 μM LPA (Sigma-Aldrich; St Louis, MO, USA) for 24 h (reporter gene analysis) or 12 h (RT–PCR). The reporter gene analysis was performed with the Dual Luciferase Assay kit (Promega).

EMSA. The nuclear extracts were mixed with 3 μg of poly (dI-dC; GE Healthcare; Buckinghamshire, England) and a radioactively labelled probe (2×10^4 c.p.m.) in a final volume of 25 μl of EMSA-binding buffer (10 mM HEPES-KOH (pH 7.8), 1 mM EDTA, 5 mM $MgCl_2$, 10% glycerol and 50 mM KCl) and incubated for 20 min at 25 °C. The protein–DNA complex was separated by 4.5% polyacrylamide gel using 0.5 × TGE (12.5 mM Tris, 95 mM glycine and 0.5 mM EDTA) as a running buffer and detected by autoradiography. In several experiments, the AhR or Arnt (H-172; Santa Cruz Biotechnology; Santa Cruz, CA, USA) antibody was added into the reactive mixture. The annealed oligo probe 5′-GATCCGGCTCTTGTCACGCAACTCCGAGCTCA-3′ includes the XRE sequence (shown here underlined). The oligo probe was radioactively labelled by T4-polynucleotide kinase (TOYOBO; Osaka, Japan) with [γ-^{32}P]ATP.

Pulse-chase analysis. For pulse-chase analysis, the transfected HEK293T cells were cultured in DMEM including [^{35}S]methionine and [^{35}S]cysteine for 60 min. Cells were then cultured in DMEM containing 2 mM non-radioactive methionine and cysteine for the indicated periods and collected in 500 μl of RIPA buffer (10 mM Tris–HCl (pH 7.5), 150 mM NaCl, 5 mM EDTA, 1% Triton X-100 and 1% deoxycholate). [^{35}S]-labelled AhR was precipitated with the haemagglutinin antibody, separated by SDS–polyacrylamide gel electrophoresis, and detected by autoradiography.

Supplementary information is available at *EMBO reports* online (http://www.emboreports.org)

ACKNOWLEDGEMENTS

We thank Dr Dirk Bohmann for providing pMT107-[His]$_6$–ubiquitin. This study was supported by grants-in-aid for scientific research from the Ministry of Education, Culture, Sports, Science, and Technology of Japan (17079006).

CONFLICT OF INTEREST

The authors declare that they have no conflict of interest.

REFERENCES

Baba T, Mimura J, Nakamura N, Harada N, Yamamoto M, Morohashi K, Fujii-Kuriyama Y (2005) Intrinsic function of the aryl hydrocarbon (dioxin) receptor as a key factor in female reproduction. *Mol Cell Biol* **25:** 10040–10051

Blatch GL, Lässle M (1999) The tetratricopeptide repeat: a structural motif mediating protein–protein interactions. *Bioessays* **21:** 932–939

Carver LA, Bradfield CA (1997) Ligand-dependent interaction of the aryl hydrocarbon receptor with a novel immunophilin homolog *in vivo*. *J Biol Chem* **272:** 11452–11456

Froidevaux MS, Berg P, Seugnet I, Decherf S, Becker N, Sachs LM, Bilesimo P, Nygard M, Pongratz I, Demeneix BA (2006) The co-chaperone XAP2 is required for activation of hypothalamic thyrotropin-releasing hormone transcription *in vivo*. *EMBO Rep* **7:** 1035–1039

Fujii-Kuriyama Y, Mimura J (2005) Molecular mechanisms of AhR functions in the regulation of cytochrome *P*450 genes. *Biochem Biophys Res Commun* **338:** 311–317

Gilman AG (1987) G proteins: transducers of receptor-generated signals. *Annu Rev Biochem* **56:** 615–649

Harper PA, Riddick DS, Okey AB (2006) Regulating the regulator: factors that control levels and activity of the aryl hydrocarbon receptor. *Biochem Pharmacol* **72:** 267–279

Kaziro Y, Itoh H, Kozasa T, Nakafuku M, Satoh T (1991) Structure and function of signal-transducing GTP-binding proteins. *Annu Rev Biochem* **60:** 349–400

Kazlauskas A, Poellinger L, Pongratz I (2000) The immunophilin-like protein XAP2 regulates ubiquitination and subcellular localization of the dioxin receptor. *J Biol Chem* **275:** 41317–41324

Kurose H (2003) $G\alpha_{12}$ and $G\alpha_{13}$ as key regulatory mediator in signal transduction. *Life Sci* **74:** 155–161

LaPres JJ, Glover E, Dunham EE, Bunger MK, Bradfield CA (2000) ARA9 modifies agonist signaling through an increase in cytosolic aryl hydrocarbon receptor. *J Biol Chem* **275:** 6153–6159

Lees MJ, Whitelaw ML (2002) Effect of ARA9 on dioxin receptor mediated transcription. *Toxicology* **181–182:** 143–146

Lees MJ, Peet DJ, Whitelaw ML (2003) Defining the role for XAP2 in stabilization of the dioxin receptor. *J Biol Chem* **278:** 35878–35888

Lin BC, Nguyen LP, Walisser JA, Bradfield CA (2008) A hypomorphic allele of aryl hydrocarbon receptor-associated protein-9 produces a phenocopy of the AHR-null mouse. *Mol Pharmacol* **74:** 1367–1371

Marty C, Browning DD, Ye RD (2003) Identification of tetratricopeptide repeat 1 as an adaptor protein that interacts with heterotrimeric G proteins and the small GTPase Ras. *Mol Cell Biol* **23:** 3847–3858

McDonough H, Patterson C (2003) CHIP: a link between the chaperone and proteasome systems. *Cell Stress Chaperones* **8:** 303–308

Meyer BK, Petrulis JR, Perdew GH (2000) Aryl hydrocarbon (Ah) receptor levels are selectively modulated by Hsp90-associated immunophilin homolog XAP2. *Cell Stress Chaperones* **5:** 243–254

Meyer BK, Pray-Grant MG, Vanden Heuvel JP, Perdew GH (1998) Hepatitis B virus X-associated protein 2 is a subunit of the unliganded aryl hydrocarbon receptor core complex and exhibits transcriptional enhancer activity. *Mol Cell Biol* **18:** 978–988

Mimura J, Fujii-Kuriyama Y (2003) Functional role of AhR in the expression of toxic effects by TCDD. *Biochim Biophys Acta* **1619:** 263–268

Petrulis JR, Kusnadi A, Ramadoss P, Hollingshead B, Perdew GH (2003) The hsp90 co-chaperone XAP2 alters importin β recognition of the bipartite nuclear localization signal of the Ah receptor and represses transcriptional activity. *J Biol Chem* **278:** 2677–2685

Pollenz RS, Dougherty EJ (2005) Redefining the role of the endogenous XAP2 and C-terminal hsp70-interacting protein on the endogenous Ah receptors expressed in mouse and rat cell lines. *J Biol Chem* **280:** 33346–33356

Roberts BJ, Whitelaw ML (1999) Degradation of the basic helix–loop–helix/Per–ARNT–Sim hoomology domain dioxin receptor via the ubiquitin/proteasome pathway. *J Biol Chem* **274:** 36351–36356

Schmidt JV, Bradfield CA (1996) Ah receptor signaling pathways. *Annu Rev Cell Dev Biol* **12:** 55–89

Sumanasekera WK, Tien ES, Turpey R, Vanden Heuvel JP, Perdew GH (2003) Evidence that peroxisome proliferator-activated receptor α is complexed with the 90-kDa heat shock protein and the hepatitis virus B X-associated protein 2. *J Biol Chem* **278:** 4467–4473

Yamaguchi Y, Katoh H, Mori K, Negishi M (2002) $G\alpha_{12}$ and $G\alpha_{13}$ interact with Ser/Thr protein phosphatase type 5 and stimulate its phosphatase activity. *Curr Biol* **12:** 1353–1358

MOLECULAR AND CELLULAR BIOLOGY, Dec. 2009, p. 6391–6400 Vol. 29, No. 24
0270-7306/09/$12.00 doi:10.1128/MCB.00337-09

Hypersensitivity of Aryl Hydrocarbon Receptor-Deficient Mice to Lipopolysaccharide-Induced Septic Shock▽†

Hiroki Sekine,[1,5] Junsei Mimura,[1,5] Motohiko Oshima,[1,5] Hiromi Okawa,[1,5] Jun Kanno,[2] Katsuhide Igarashi,[2] Frank J. Gonzalez,[3] Togo Ikuta,[4] Kaname Kawajiri,[4] and Yoshiaki Fujii-Kuriyama[1,5]*

The Center for Tsukuba Advanced Research Alliance and Institute of Basic Medical Sciences, University of Tsukuba, 1-1-1 Tennoudai, Tsukuba 305-8577, Japan[1]; Division of Molecular Toxicology, National Institute of Health Sciences, 1-18-1 Kamiyoga, Setagaya-ku, Tokyo 158-8501, Japan[2]; Laboratory of Metabolism, Center for Cancer Research, National Cancer Institute, National Institutes of Health, Bethesda, Maryland 20892[3]; Research Institute for Clinical Oncology, Saitama Cancer Center, 818 Komuro, Ina-machi, Kitaadachi-gun, Saitama 362-0806, Japan[4]; and SORST, Japan Science and Technology Agency, 4-1-8 Honcho, Kawaguchi, 332-0012, Japan[5]

Received 16 March 2009/Returned for modification 2 May 2009/Accepted 11 September 2009

Aryl hydrocarbon receptor (AhR), a ligand-activated transcription factor, is known to mediate a wide variety of pharmacological and toxicological effects caused by polycyclic aromatic hydrocarbons. Recent studies have revealed that AhR is involved in the normal development and homeostasis of many organs. Here, we demonstrate that AhR knockout (AhR KO) mice are hypersensitive to lipopolysaccharide (LPS)-induced septic shock, mainly due to the dysfunction of their macrophages. In response to LPS, bone marrow-derived macrophages (BMDM) of AhR KO mice secreted an enhanced amount of interleukin-1β (IL-1β). Since the enhanced IL-1β secretion was suppressed by supplementing Plasminogen activator inhibitor-2 (Pai-2) expression through transduction with Pai-2-expressing adenoviruses, reduced Pai-2 expression could be a cause of the increased IL-1β secretion by AhR KO mouse BMDM. Analysis of gene expression revealed that AhR directly regulates the expression of Pai-2 through a mechanism involving NF-κB but not AhR nuclear translocator (Arnt), in an LPS-dependent manner. Together with the result that administration of the AhR ligand 3-methylcholanthrene partially protected mice with wild-type AhR from endotoxin-induced death, these results raise the possibility that an appropriate AhR ligand may be useful for treating patients with inflammatory disorders.

The aryl hydrocarbon receptor (AhR) is a member of the basic helix-loop-helix/Per-Arnt-Sim homology superfamily and is involved in the induction of drug-metabolizing enzymes and the susceptibility of cells to a variety of cytotoxicities induced by dioxins (9). AhR is a ligand-activated transcription factor activated by polycyclic aromatic hydrocarbons (PAHs), such as 3-methylcholanthrene (3MC) and 2′,3′,7′,8′-tetrachlorodibenzo-*p*-dioxin (TCDD). Under normal conditions, AhR exists in the cytoplasm in a complex with Hsp90, XAP2, and p23 (22). After binding a ligand, AhR translocates into the nucleus where it dimerizes with its partner molecule, AhR nuclear translocator (Arnt), and acts as a transcriptional activator to regulate the expression of target genes, such as those expressing drug-metabolizing cytochrome P450 (Cyp1a1, 1a2, and 1b1) and NAD(P)H: quinone oxidoreductase (Nqo), by binding to xenobiotic response element (XRE) sequences in their promoter regions (9). By using AhR knockout (AhR KO) mice, it has been demonstrated that AhR is essential not only for the induction of drug-metabolizing enzymes but also for most, if not all, of the toxicological effects caused by TCDD, including immunosuppression, thymic atrophy, teratogenesis, and hyperplasia (6, 7, 17, 24), the mechanisms for which are largely unknown. Recently, careful investigation into the loss of functions in AhR KO mice has also revealed that AhR is involved in the normal development of several organs, including the liver, heart, vascular tissues, and reproductive organs (1, 2, 6, 8, 15, 24). In addition, AhR has been found to play a key role in the differentiation of regulatory T cells Treg, Th17, and Th1 from naive CD4 T cells by regulating their expression of Foxp3 or by as-yet-unknown mechanisms (14, 20, 23, 32). From these studies, one of the general features of AhR that begins to emerge is that it serves as a multifunctional regulator in a large number of areas, ranging from drug metabolism to innate immunity for protection against invasive xenobiotics. In the work presented here, we demonstrated that AhR KO mice were hypersensitive to lipopolysaccharide (LPS)-induced septic shock, mainly due to the dysfunction of their macrophages. AhR KO mouse macrophages secreted an enhanced amount of interleukin-1β (IL-1β) in response to LPS treatment and had markedly reduced Plasminogen activator inhibitor-2 (Pai-2) mRNA concentrations, as revealed by DNA microarray analysis. Pai-2 was reported to be a negative regulator of IL-1β secretion through its inhibition of caspase-1 (10), suggesting that the enhanced secretion of IL-1β by AhR KO macrophages in response to LPS may have been due to the reduced level of Pai-2. We showed that AhR directly regulates the expression of inhibitory Pai-2, in an LPS-dependent manner, through a mechanism involving NF-κB but not Arnt.

* Corresponding author. Present address: 5-18-7 Honkomagome, Bunkyo-ku, Tokyo 113-0021, Japan. Phone and fax: 3-3941-2200. E-mail: y.k_fujii@nifty.com.

† Supplemental material for this article may be found at http://mcb.asm.org/.

▽ Published ahead of print on 12 October 2009.

MATERIALS AND METHODS

Mice. AhR knockout (AhR KO) mice were generated as described previously (17). These mice were back-crossed with C57BL/6J mice at least 10 times. Age-matched mice (10 weeks) were intraperitoneally injected with 20 mg of

LPS/kg of body weight. Mice with floxed *Arnt* (30) and *AhR* (Jackson laboratory) alleles were crossed to LysM Cre mice to specifically delete these genes in their macrophages. $AhR^{flox/-}$ and $AhR^{flox/-}$::LysM Cre mice were generated by mating $AhR^{flox/flox}$::LysM Cre and $AhR^{-/-}$ (AhR KO) mice. These age-matched mice (9 to 11 weeks old) were intraperitoneally injected with 25 mg LPS/kg. Mouse survival was checked every 6 or 12 h. 3MC (Wako, Osaka) at 10 μl (4 mg/ml 3MC)/g of body weight or 10 μl corn oil/g was intraperitoneally injected. After 2 h, each mouse was intraperitoneally injected with 30 mg LPS/kg. LPS (from *Escherichia coli* 0111:B4) was purchased from Sigma.

Preparation of macrophages. Bone marrow cells were obtained from the femurs of 8- to 12-week-old mice. The bone marrow-derived macrophages (BMDM) used for each experiment were isolated by culturing bone marrow cells in the presence of 10 ng/ml granulocyte-macrophage colony-stimulating factor (PeproTech) for 7 days and washing the attached cells with phosphate-buffered saline (PBS) three times. For cytokine assays, washed cells were collected with a scraper, plated at 2×10^6 cells/ml in 96-well plates, and cultured with 10 ng/ml LPS for 8 h.

For isolation of peritoneal exudate macrophages (PEMs), mice were intraperitoneally injected with 2 ml of 4% thioglycolate. Peritoneal cells were isolated from exudates of the peritoneal cavity 3 days after injection, incubated for 3 h in appropriate plates, and washed with PBS. The adherent cells were used for experiments.

Measurement of cytokines. Mice were intraperitoneally injected with 20 mg/kg LPS and bled 2 h after injection. Plasma concentrations of IL-1β, tumor necrosis factor alpha (TNF-α), IL-6, gamma interferon (IFN-γ), IL-12, and IL-18 were determined by enzyme-linked immunosorbent assay (ELISA) (Biosource). BMDM of mice with wild-type AhR (AhR WT mice) and AhR KO at 2×10^6 cells/ml were incubated with 10 ng/ml LPS for 8 h, and their culture supernatants were assessed for cytokines using mouse TNF-α and IL-1β ELISAs (Biosource).

Cell culture. All cells were maintained in RPMI medium (Sigma) supplemented with 10% fetal bovine serum (HyClone) and penicillin/streptomycin (Gibco) under 5.0% CO_2 at 37°C.

Caspase inhibitors. BMDM of AhR KO mice at 2×10^6 cells/ml were incubated with dimethyl sulfoxide (DMSO) or 80 μM Z-YVAD-FMK (caspase-1 inhibitor VI; Merck) or 100 μM Z-VAD-FMK (caspase inhibitor VI; Merck) for 30 min before LPS (10 ng/ml) stimulation. The BMDM were incubated for 8 h, and their culture supernatants were assessed for cytokines using a mouse IL-1β ELISA (Biosource).

Virus infections. Adenoviruses expressing green fluorescent protein (GFP), human Pai-2 (hPai-2), and human Bcl-2 (hBcl-2) were purchased from Vector Biolabs (Philadelphia). BMDM from AhR KO mice were infected for 12 h with adenoviruses expressing GFP, hPai-2, and hBcl-2 at a multiplicity of infection of 100. Infected BMDM were washed with PBS, followed by 12 h of incubation. As it was reported that adenoviral vectors enhanced IL-1β secretion in macrophages (19), IL-1β levels were investigated in these incubation supernatants by ELISA. At this point, no IL-1β was observed in the supernatants. Therefore, the cells were washed, collected with a scraper, and plated at 2×10^6 cells/ml in 96-well plates. The cells were treated with 10 ng/ml of LPS for an additional 8 h.

Retroviral infection was performed as follofws: pQC-mAhR, a cloned murine AhR (mAhR) fragment in pQCXIN (Clontech), and pQCXLN for LacZ expression (as a control) were transfected into PT67 cells that were then cultured for 24 h. The culture medium was replaced with fresh medium, and the culture was continued for an additional 24 h. This culture medium was used as the retrovirus particle source.

Microarray analysis. Total RNA samples were purified using Isogen before being processed and hybridized to Affymetrix mouse genome 430 2.0 arrays (Affymetrix). The experimental procedures for the GeneChip analyses were performed according to the Affymetrix technical manual.

Generation of stable transformant cell lines. ANA-1 cells were the kind gift of L. Varesio (3). ANA-1 cells were transduced with LacZ- or AhR-expressing retroviruses in a suspension with 8 mg/ml of Polybrene. One day after infection, the infected cells were replated and incubated in a selection medium containing 0.5 mg/ml of Geneticin (Gibco).

Plasmids. pcDNA3-p65 and pcDNA3-AhR were generated by inserting AhR and p65 cDNA fragments, excised from pBS-mAhR and pBS-mp65 (murine p65), into the pcDNA3 vector. The 2.7-kb fragment upstream of the Pai-2 transcription start site was generated by PCR (primers 5′-gaagcttGGGTTGCA GATCCCTTTAGC-3′ and 5′-ccatggtggCTGACACACAGGAAATGCTTC-3′; lowercase indicates restriction site sequences for cloning), using a BAC vector carrying the Pai-2 gene as a template, and then cloned into the pBS vector. After sequencing, the construct was cleaved with HindIII/NcoI, and the isolated insert was cloned into the HindIII/NcoI-digested pGL4.10 (Promega) to produce pGL4-Pai-2 (−2.7 kb). The 0.8-kb fragment upstream of the Pai-2 transcription start site was generated by PCR (primers 5′-ggaattcGAGAAGTGATCTGGTA GATG-3′ and 5′-ccatggtggCTGACACACAGGAAATGCTTC-3′) using pGL4-Pai-2 (−2.7 kb) as a template and cloned into the pBS vector. After sequencing, the construct was cleaved with HindIII/NcoI, and the isolated insert was cloned into the HindIII/NcoI-digested pGL4.10 (Promega) to produce pGL4-Pai-2 (−0.8 kb). pGL4-Pai-2 (−0.55 kb) was produced by cleaving pGL4-Pai-2 (−2.7 kb) with NdeI/EcoRV. pGL4-Pai-2 (−0.1 kb) was generated in a similar manner, using primers 5′-GATGTCTTTATGAGTAAAATGTTGAATCA-3′ and 5′-cca tggtggCTGACACACAGGAAATGCTTC-3′. pGL4-Pai-2 (−0.55 kb C/EBPβ mutant) was generated by site-directed mutagenesis using a Sculptor in vitro mutagenesis system (Amersham) with pGL4-Pai-2 (−0.55 kb) as a template and primer pair 5′-GATTTAAAATTGGAAAggGCTAAATTCTTGAATTTTGAA TGACATCAC-3′ and 5′-GTGATGTCATTCAAAATTCAAGAATTTAGCcc TTTCCAATTTTAAATC-3′.

RNA preparation and reverse transcription PCR (RT-PCR). Total RNA was prepared using Isogen (Nippon Gene, Tokyo) according to the manufacturer's protocol. cDNA synthesis from 1 μg of total RNA was carried out using SuperScript II reverse transcriptase (Invitrogen, United States). Real-time PCR was performed using an ABI7300 real-time PCR system (Applied Biosystems) and Platinum SYBR green quantitative PCR SuperMix (Invitrogen, United States). Each sample was normalized to the expression of β-actin as a control. The primer sequences were as follows: Pai-2, 5′-GCATCCACTGGCTTGGAA-3′ and 5′-GGGAATGTAGACCACAACATCAT-3′; Bcl-2, 5′-GTGGTGGAGGA ACTCTTCAGGGATG-3′ and 5′-GGTCTTCAGAGACAGCCAGGAGAAAT C-3′; AhR, 5′-TTCTATGCTTCCTCCACTATCCA-3′ and 5′-GGCTTCGTCC ACTCCTTGT-3′; Arnt, 5′-GGACGGTGCCATCTCGAC-3′ and 5′-CATCTG GTCATCATCGCATC-3′; Mmp-8, 5′-CCACACACAGCTTGCCAATGCC T-3′ and 5′-GGTCAGGTTAGTGTGTGTCCACT-3′; Nqo1, 5′-TTTAGGGTC GTCTTGGCAAC-3′ and 5′-AGTACAATCAGGGCTCTTCTCG-3′; AhR repressor, 5′-CCTGTCCCGGGATCAAAGATG-3′ and 5′-CTCACCACCAG AGCGAAGCCATTGA-3′; IL-1β, 5′-CTGAAGCAGCTATGGCAACT-3′ and 5′-GGATGCTCTCATCTGGACAG-3′; TNF-α, 5′-CTGTAGCCCACGTCGT AGC-3′ and 5′-TTGAGATCCATGCCGTTG-3′; Cox-2, 5′-GCATTCTTTGCC CAGCACTT-3′ and 5′-AGACCAGGCACCAGACCAAAG-3′; β-actin, 5′-GA CAGGATGCAGAAGGAGAT-3′ and 5′-TTGCTGATCCACATCTGCTG-3′; hPai-2, 5′-CCCAGAACCTCTTCCTCTCC-3′ and 5′-CATTGGCTCCCACTT CATTA-3′; and hBcl-2, 5′-GTGTGTGGAGAGCGTCAACC-3′ and 5′-GAGA CAGCCAGGAGAAATCAAA-3′.

Reporter assays. All luciferase assays were performed using a dual-luciferase reporter assay system according to the manufacturer's protocol (Promega), with some modifications. RAW 264.7 cells (2.0×10^4 cells/well) were plated in 24-well plates 24 h prior to transfection. Cells were cotransfected with 100 ng pGL4-Pai-2 (various lengths in kilobases) (see "Plasmids"), 1 ng *Renilla* luciferase (as an internal control), and 1 ng pcDNA3-p65 and/or pcDNA3-AhR using FuGENE HD transfection reagent (Roche) according to the manufacturer's protocol. All cells were incubated for 12 h at 37°C after transfection, treated with 10 ng/ml LPS, and incubated for an additional 6 h.

Co-IP assays. AhR WT PEMs or transfected 293T cells were washed with ice-cold PBS, followed by buffer containing 20 mM HEPES, pH 7.4, 125 mM NaCl, 1% Triton X-100, 10 mM EDTA, 2 mM EGTA, 2 mM Na_3VO_4, 50 mM sodium fluoride, 20 mM $ZnCl_2$, 10 mM sodium pyrophosphate (31). The cells were harvested by scraping, centrifuged at 5,000 rpm at 4°C for 5 min, and suspended in immunoprecipitation (IP) buffer containing a protease inhibitor cocktail (Roche). The cells were vortexed and placed on ice for 10 min. The samples were then centrifuged at 15,000 rpm for 5 min at 4°C, and the supernatants were saved as whole-cell lysates.

The prepared whole-cell lysate (250 μl) was incubated with anti-immunoglobulin G, anti-AhR antibody, or anti-p65 for 2 h at 4°C. The reaction mixture was supplemented with 20 μl of protein A-agarose beads (Amersham). After being incubated for an additional 1 h at 4°C, the beads were washed three times with IP buffer containing protease inhibitor cocktail and resuspended in sodium dodecyl sulfate (SDS) sample buffer. The coimmunoprecipitated proteins were resolved by SDS-polyacrylamide gel electrophoresis (PAGE), and Western blot analysis was performed.

ChIP assays. Chromatin IP (ChIP) assays were performed with PEMs from AhR WT and AhR KO mice. PEMs were stimulated with 10 ng/ml LPS for 60 min and then fixed with formaldehyde for 10 min. The cells were lysed and sheared by sonication. The lysis solution was incubated with immunoglobulin G or preimmune serum and protein A-agarose for 2 h to remove nonspecific DNA binding. The solution was incubated overnight with a specific antibody, followed by incubation with protein A-agarose saturated with salmon sperm DNA. Precipitated DNA was analyzed by real-time PCR using primer pair 5′-GGAAGT TCCCTGAGGCTTATAGG-3′ and 5′-ATGGAAGCACATACATAAGAACA

TGG-3′ for the NF-κB binding site of Pai-2, 5′-TGAGTGTGAGTGGTGCAG ATTAC-3′ and 5′-CCTCCCACACAGCTCTTTTTTC-3′ for mPai-2 TATA, 5′-CGGAGGGTAGTTCCATGAAA-3′ and 5′-CAGGCTTTTACCCACGCAA A-3′ for the NF-κB binding site of mCox2, and 5′-CGCAACTCACTGAAGC AGAG-3′ and 5′-TCCTTCGTGAGCAGAGTCCT-3′ for mCox-2 TATA. The antibodies used were as follows: anti-AhR serum, preimmune serum, anti-p65, and anti-PolII antibodies (Santa Cruz).

Western blot analyses. Cells were dissolved in SDS sample buffer, and proteins were separated by SDS-PAGE for Western blot analysis. The proteins were then transferred to polyvinylidene difluoride membranes and blocked in 3% skim milk for 30 min. Each antibody was used as a primary reagent, and after being washed three times with Tris-borate-EDTA containing 0.1% Triton X-100, membranes were incubated with species-specific horseradish peroxidase-conjugated secondary antibody (Zymed). The protein-antibody complexes were visualized by using an enhanced chemiluminescence detection system (Amersham) according to the manufacturer's recommendations. Nuclear extracts were prepared by a standard method (25). The antibodies used were as follows: anti-Arnt serum (28); anti-AhR (Biomol); anti-Pai-2, anti-p65, and antilamin antibodies (Santa Cruz); and antitubulin antibody (Sigma).

RESULTS

High susceptibility of AhR-deficient mice to LPS-induced endotoxin shock. To investigate the function of AhR in acute inflammation in vivo, we performed studies of experimental LPS-induced endotoxin shock. For these studies, 10-week-old AhR WT and AhR KO mice were injected intraperitoneally with 20 mg/kg LPS. After 24 h, while all of the AhR WT mice survived, most of the AhR KO mice (80%) had died (Fig. 1A). These data indicate that AhR-deficient mice were highly susceptible to LPS-induced endotoxin shock. To explain the increased sensitivity of AhR KO mice to septic shock, the plasma concentrations of several inflammatory cytokines were measured 2 h after LPS challenge. Consistent with the enhanced susceptibility of AhR KO mice to the LPS treatment, AhR KO mice had marked increases in plasma IL-1β, IL-18, and TNF-α levels ($P < 0.001$), with modest increases in IL-6 and IFN-γ (Fig. 1B). In contrast, there was no difference in plasma IL-12p70 levels (Fig. 1B). Administration of 3MC, an AhR ligand, before LPS treatment (30 mg/kg) made the AhR WT mice significantly more resistant to septic shock than the mice that were not treated with 3MC ($P = 0.002$) (Fig. 1C). Together with the fact that there was essentially no effect of 3MC on AhR KO mice, these results suggested that activated AhR could play an anti-inflammatory role.

Increased susceptibility of mice with AhR KO macrophages to LPS-induced endotoxin shock. Since macrophages play an important role in sensitivity to LPS toxicity, we generated mice with macrophages deficient in AhR ($AhR^{flox/-}$::LysM Cre [ΔAhR Mac] mice) to evaluate the contribution of macrophages to the LPS hypersensitivity of AhR KO mice. When ΔAhR Mac and control mice ($AhR^{flox/-}$) were injected intraperitoneally with 25 mg/kg LPS, most of the ΔAhR Mac mice (80%) had died at 48 h after LPS challenge, while 60% of the control mice survived ($P = 0.03$) (Fig. 2A). Together with the previous results, these data showed that dysfunctional AhR-deficient macrophages are one of the main causes of LPS hypersensitivity in AhR KO mice.

Elevated IL-1β secretion from AhR KO BMDM in response to LPS. To further investigate the cause of the aberrant cytokine secretion by LPS-challenged AhR KO mice, we next asked if there were any differences in the production of proinflammatory cytokines by AhR WT and AhR KO mouse

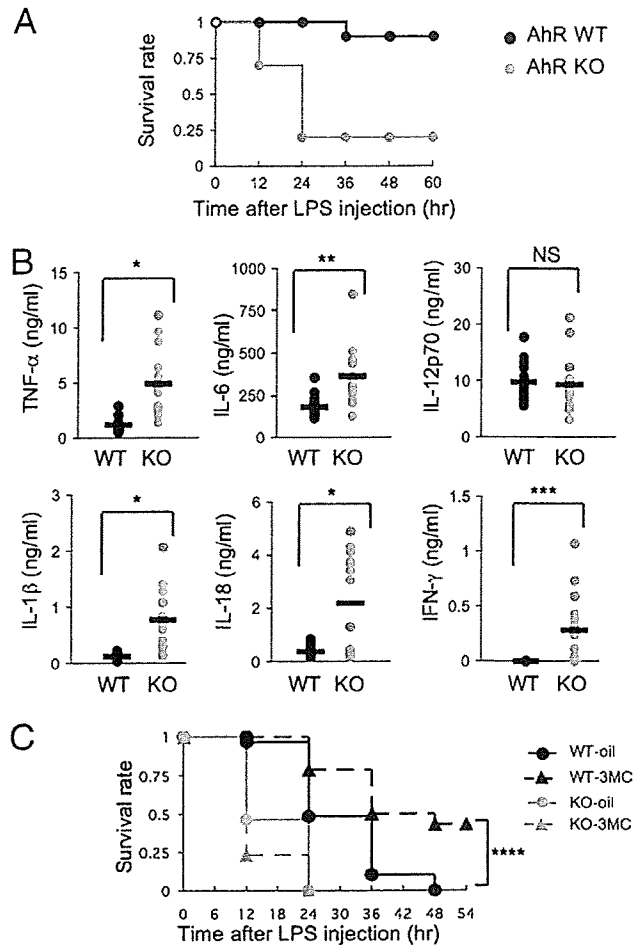

FIG. 1. High susceptibility of AhR KO mice to LPS-induced endotoxin shock. (A) Survival of AhR WT and AhR KO mice ($n = 10$) after LPS challenge (20 mg/ml). (B) TNF-α, IL-6, IL-12p70, IL-1β, IL-18, and IFN-γ plasma levels 2 h after LPS challenge (20 mg/ml). Horizontal bars show the mean results. (C) Partial protection of AhR WT mice from septic shock by intraperitoneal injection of 3MC at 2 h before LPS challenge (30 mg/ml) and survival of corn oil-injected mice. AhR WT-oil, $n = 29$; AhR WT-3MC, $n = 28$; AhR KO-oil, $n = 13$; AhR KO-3MC, $n = 13$. *, $P < 0.001$; **, $P = 0.001$; ***, $P < 0.005$; ****, $P = 0.002$; NS, not significant.

BMDM in response to LPS stimulation. Macrophages from the bone marrow of AhR WT and AhR KO mice were challenged with 10 ng/ml LPS for 8 h, and then the levels of TNF-α and IL-1β in the culture medium were assessed by ELISA. Compared to the levels in AhR WT BMDM, the levels of IL-1β secretion by AhR KO BMDM were markedly elevated, along with slight increases in TNF-α, in response to LPS treatment ($P < 0.001$) (Fig. 2B, left). However, IL-1β mRNA levels were not altered between AhR WT and AhR KO BMDM (Fig. 2C, left). These data indicated that AhR deficiency markedly increased IL-1β accumulation due to its enhanced secretion rather than its increased synthesis.

Expression of AhR-dependent genes in macrophages. We next performed microarray analysis of AhR WT and AhR KO mouse macrophages to comprehensively investigate the AhR-

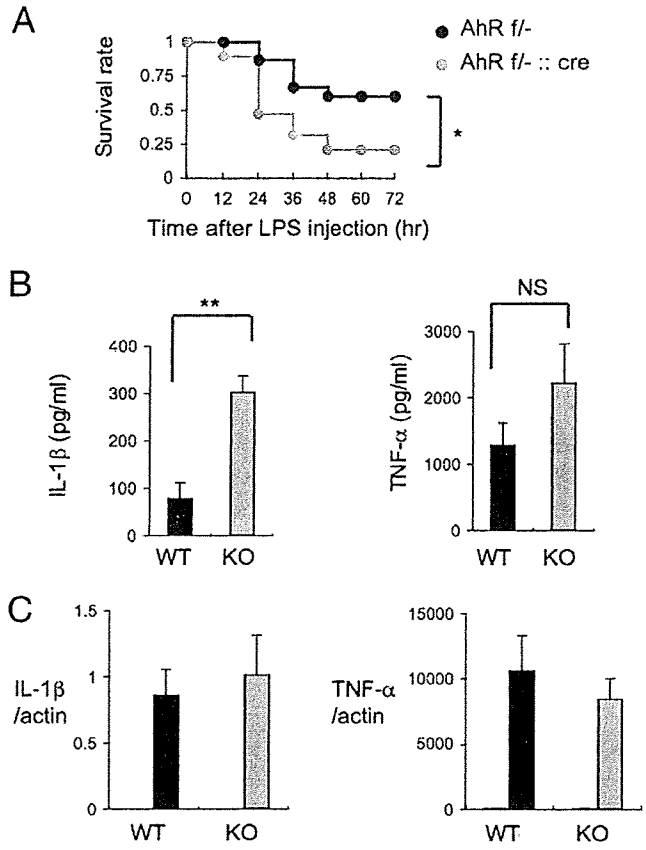

FIG. 2. LPS induces abnormal secretion of IL-1β by BMDM from AhR KO mice. (A) Survival of $AhR^{flox/-}$ (AhR f/−; $n = 15$) and $AhR^{flox/-}$::LysM Cre (AhR f/−::cre; $n = 19$) mice after LPS challenge (25 mg/ml). (B) IL-1β and TNF-α levels in the culture supernatants of AhR WT and AhR KO BMDM 8 h after LPS stimulation (10 ng/ml) ($n = 4$). (C) Relative expression levels of IL-1β and TNF-α mRNA 4 h after LPS stimulation (10 ng/ml) of AhR WT and AhR KO BMDM. Gray and black bars show results with LPS; white bars show results for untreated cells. Error bars show standard deviations. *, $P = 0.03$; **, $P < 0.001$; NS, not significant.

dependent changes in gene expression that were related to IL-1β secretion (Table 1). Among the genes whose expression was reduced in AhR KO macrophages, we noted the markedly reduced levels of expression of the Pai-2 and Bcl-2 genes. These genes were significant because they had been reported to negatively regulate IL-1β secretion by inhibiting the activity of caspase-1 (5, 10). Consistent with the notion that the enhanced secretion of IL-1β is due to the activation of caspase-1, treatment with the caspase inhibitors Z-YVAD-FMK and Z-VAD-FMK markedly reduced the secretion of IL-1β in AhR KO BMDM (Fig. 3A). To confirm their reduced expression in AhR KO BMDM, Pai-2 and Bcl-2 mRNA expression levels were determined by real-time RT-PCR in AhR WT and AhR KO BMDM (Fig. 3B). Figure 3B shows that Pai-2 and Bcl-2 mRNA expression levels were clearly reduced in AhR KO BMDM. To investigate whether the increased IL-1β secretion in AhR KO BMDM was due to their reduced Pai-2 and Bcl-2 expression, the expression of these proteins was supplemented in AhR KO BMDM by infection with adenoviral vectors expressing hPai-2 and hBcl-2 (Fig. 3D). The efficiency of the adenoviral gene transfer, as monitored by the expression of GFP, was estimated to be >90% (data not shown). Compared with control adenoviral expression of GFP, transfer of the hPai-2 gene into AhR KO BMDM significantly inhibited LPS-induced secretion of IL-1β (Fig. 3C), but almost no effect was observed with Bcl-2 expression. Bcl-2 has been reported to suppress IL-1β secretion that is specifically processed through the NALP1 complex and regulated by muramyl dipeptide, which is usually a contaminant in commercial LPS (5). These results suggested that the enhanced IL-1β secretion in response to LPS was due not to processing through the NALP1 complex (5) but to processing through the NALP3 complex, an inflammasome-containing caspase-1 regulated by LPS (16), and that decreased Pai-2 expression is at least one of the causes for the increased IL-1β secretion by AhR KO BMDM after LPS treatment.

Arnt is not required for enhancement of LPS-induced Pai-2 expression by AhR. It has been reported that LPS stimulation induces Pai-2 expression (21, 26). Figure 4A and B show that the induction of both Pai-2 mRNA and protein expression was remarkably reduced in AhR KO macrophages compared with the levels in AhR WT macrophages. Interestingly, AhR mRNA and protein expression levels were also induced by LPS stimulation (Fig. 4A and B). In response to various PAHs, AhR is known to act, in most cases, as a transcriptional activator, in heterodimer formation with Arnt. Although the mouse Pai-2 promoter does not have any obvious XRE sequences (GCGTG) in its regions 5 kb upstream and down-

TABLE 1. Decreased gene expression in AhR KO PEMs revealed by cDNA microarray analysis

Fold change	Value for		Gene name	Gene product
	WT PEMs	KO PEMs		
14.0	0.561	0.040	*Gsta3*	Glutathione *S*-transferase alpha 3
10.2	7.826	0.767	*Pai-2*	Plasminogen activator inhibitor-2
5.5	9.354	1.700	*Cyp1b1*	Cytochrome P450, family 1, subfamily b, polypeptide 1
4.6	0.206	0.045	*Nkrf*	NF-κB repressing factor
3.6	1.922	0.541	*Cxcl5*	Chemokine (C-X-C motif) ligand 5
3.1	13.670	4.444	*Mmp8*	Matrix metallopeptidase 8
2.9	1.406	0.489	*Cxcl13*	Chemokine (C-X-C motif) ligand 13
2.6	2.111	0.800	*Lrrc27*	Leucine-rich repeat-containing 27
2.5	3.466434	1.394728	*Ctgf*	Connective tissue growth factor
2.2	3.849141	1.722473	*Mcoln3*	Mucolipin 3
2.2	1.204793	0.550093	*Nqo1*	NAD(P)H dehydrogenase, quinone 1
2.0	6.96623	3.453017	*Ier3*	Immediate early response 3
2.0	0.596479	0.294062	*Bcl2*	B-cell leukemia/lymphoma 2